Effect of elevated CO_2 on organic matter pools and fluxes in a summer Baltic Sea plankton community

A. J. Paul[1*], L. T. Bach[1], K.-G. Schulz[1,2], T. Boxhammer[1], J. Czerny[1], E. P. Achterberg[1,3], D. Hellemann[1,4], Y. Trense[1,6], M. Nausch[5], M. Sswat[1], U. Riebesell[1]

[1] {GEOMAR Helmholtz Centre for Ocean Research Kiel, Düsternbrooker Weg 20, 24105 Kiel, Germany}

[2] {Southern Cross University, Military Road, East Lismore, NSW 2480, Australia}

[3] {National Oceanography Centre Southampton, European Way, University of Southampton, Southampton SO14 3ZH, United Kingdom}

[4] {Department of Environmental Sciences, University of Helsinki, PL 65 00014 Helsinki, Finland}

[5] {Leibniz Institute for Baltic Sea Research, Seestrasse 15, 18119 Rostock, Germany}

[6] {now at: Comprehensive Centre for Inflammation Medicine, University of Lübeck, Ratzeburger Allee 160, 23538 Lübeck, Germany}

*Correspondence to: A. J. Paul (apaul@geomar.de)

Abstract

Ocean acidification is expected to influence plankton community structure and biogeochemical element cycles. To date, the response of plankton communities to elevated CO_2 was studied primarily during nutrient-stimulated blooms. In this CO_2 manipulation study, we used large-volume (~55 m^3) pelagic in situ mesocosms to enclose a natural summer, post spring-bloom plankton assemblage in the Baltic Sea to investigate the response of organic matter pools to ocean acidification. The carbonate system in the six mesocosms was manipulated to yield average fCO_2 ranging between 365 and ~1230 µatm with no adjustment of naturally available nutrient concentrations. Plankton community development and key biogeochemical element pools were subsequently followed in this nitrogen-limited ecosystem over a period of seven weeks. We observed higher sustained chlorophyll *a* and particulate

matter concentrations (~25 % higher) and lower inorganic phosphate concentrations in the water column in the highest fCO_2 treatment (1231 µatm) during the final two weeks of the study period (Phase III), when there was low net change in particulate and dissolved matter pools. Size-fractionated phytoplankton pigment analyses indicated that these differences were driven by picophytoplankton (<2 µm) and were already established early in the experiment during an initial warm and more productive period with overall elevated chlorophyll *a* and particulate matter concentrations. However the influence of picophytoplankton on bulk organic matter pools was masked by high biomass of larger plankton until Phase III when the contribution of the small size fraction (<2 µm) increased to up to 90 % of chlorophyll *a*. In this phase, CO_2-driven increase in water column particulate carbon did not lead to enhanced sinking material flux but was instead reflected in increased dissolved organic carbon concentrations. Hence ocean acidification may induce changes in organic matter partitioning in the upper water column during the low nitrogen summer period in the Baltic Sea.

1 Introduction

The Baltic Sea is a semi-enclosed, brackish epicontinental sea with a substantial freshwater catchment area which is approximately four times larger than the water body itself. In addition, the Baltic Sea has limited and infrequent saline deep water inputs from the North Sea through the Danish Straits which form an important oxygen supply for the Baltic Sea bottom waters. Weak circulation, vertical mixing and water mass exchange in the Baltic Sea leads to strong horizontal and vertical salinity gradients (surface waters from north (< 5) to south (~20) Baltic, and surface (~7) to deep (~12) at station BY15 at Gotland Deep (The International Council for the Exploration of the Sea, 2014)). Consequently, the enclosed nature of the water body and minimal water exchange mean that terrestrial and anthropogenic activities have a considerable influence on water quality, biogeochemistry and ecosystems in the Baltic Sea.

Global change is expected to have pronounced effects on the physical and chemical conditions in the Baltic Sea. Warming, decreasing pH, and increasing freshwater inputs are expected to affect primary productivity and decrease oxygen concentrations in the deeper basins (HELCOM, 2013). In combination with higher nutrient loads from changes in agricultural activity, this may lead to increased hypoxia or even anoxia in sub-surface waters (Meier et al., 2011) with feedbacks on biogeochemical element cycles (Sutton et al., 2011),

and ecosystem structure and functioning particularly at higher trophic levels (Ekau et al., 2010; Turner, 2001; Wu, 2002). Changes in the Baltic Sea environment have already been detected. Regular monitoring of the Baltic Sea over the past 100 years has indicated higher rates of temperature increase (0.08 to 0.11°C per decade) than the global average, along with a 20 % decrease in annual maximum ice extent (HELCOM, 2013). Observed shifts in the spring and summer phytoplankton community dynamics have been primarily associated with warming in northern Baltic Sea regions over the past three decades (Suikkanen et al., 2013).

Ocean acidification is another anthropogenic process of potential relevance for Baltic plankton communities. As CO_2 dissolves in seawater, the carbonate system shifts with an associated decrease in pH. Ocean acidification therefore adds to the decrease in seawater pH as a result of nitrogen and sulphate deposition in the form of acid rain (Doney et al., 2007). Between 1993 and 2012, pH in the Baltic Proper decreased on the order of 0.1 pH units (The International Council for the Exploration of the Sea, 2014) which is more than two times faster than observed in the Pacific Ocean (~0.04 pH decrease between 1992 and 2012 in surface 30 m, Station ALOHA, Hawaii Ocean Time-Series (Dore et al., 2009)). Changes in fCO_2 and pH influence phytoplankton physiology, growth rates, and carbon fixation with some phytoplankton functional groups, such as calcifying organisms, more sensitive than others such as diatoms (Riebesell and Tortell, 2011; Rost et al., 2008). Thus the relative fitness of each functional group determines the response of the plankton community as a whole. Changes in physiological processes in phytoplankton on a cellular level can cascade through trophic levels and induce shifts in the structure of the planktonic food web.

To date, the majority of ocean acidification experiments have utilised nutrient replete starting conditions or added nutrients to investigate effects of high CO_2 on plankton communities and biogeochemical cycles (nutrient replete/addition e.g. Biswas et al., 2012; Engel et al., 2005, 2008, 2014; Feng et al., 2010; Hama et al., 2012; Hare et al., 2007; Hopkins et al., 2010; Hopkinson et al., 2010; Hoppe et al., 2013; Kim et al., 2006; Nielsen et al., 2010, 2011; Richier et al., 2014; Rossoll et al., 2013; Schulz et al., 2008, 2013; Tatters et al., 2013a, 2013b; Yoshimura et al., 2013, 2014) vs. (nutrient deplete e.g. Law et al., 2012; Lomas et al., 2012; Losh et al., 2012; Yoshimura et al., 2010). These studies mimic the productive spring bloom where nutrient concentrations are relatively high and relatively low light levels initially limit phytoplankton growth. However for considerable parts of the year, the opposite is the case. Growth is not limited by light but by nutrient concentrations and biomass tends to be

low. This is also the case during summer in the Baltic Sea. Here, a diatom-dominated spring bloom in April/May usually draws down dissolved inorganic nutrients so that concentrations remain low from early summer. Diazotrophic filamentous cyanobacteria then commonly bloom in July and August when surface water temperatures peak, calm weather conditions induce water column stratification and low nitrogen in a bioavailable form limits growth in the non-diazotrophic phytoplankton (Gasiūnaitė et al., 2005; Kanoshina et al., 2003; Stal et al., 1999).

We undertook a pelagic in situ mesocosm study on a summer Baltic Sea plankton community to investigate the response of this low nutrient ecosystem to projected changes in fCO_2. Using this approach, many different trophic levels from bacteria and viruses through to zooplankton can be investigated over extended periods of time. Using the KOSMOS mesocosm system (Kiel Off-Shore Mesocosms for future Ocean Simulations, Riebesell et al. (2013)), we were able to enclose large volumes containing whole plankton communities with a low level of disturbance and thereby utilising natural variability in light and temperature.

2 Methods

2.1 Study area, deployment site, and mesocosm set-up

On 12 June 2012 (day -10 = *t-10*, 10 days before CO_2 manipulation), nine floating, pelagic mesocosms (Fig. 1, KOSMOS, volume ~ 55 m^3) were deployed and moored at 59° 51.5’ N, 23° 15.5’ E in the Tvärminne Storfjärden, an open archipelago area on the eastern side of the Hanko peninsula on the south-west coast of Finland (Fig. 2). The water depth at the mooring site was approximately 30 m. The bottom ends of the mesocosm bags were lowered to a depth of 17 m below the surface to enclose the plankton community with minimal disturbance to the water column. A mesh of 3 mm was attached to the top, which was submerged ~0.5 m below the surface, and bottom of the bag, at 17 m deep, to exclude any large organisms or particles with patchy distribution in the water column. Initially the mesocosm bags were kept open and covered with only the 3 mm nets at the top and bottom openings for five days to allow for rinsing of the mesocosm bags water and free exchange of plankton (< 3 mm). On *t-7*, the nets were removed, sediment traps (2 m long, Fig. 1) were then attached to close the bottom of the mesocosms and the top ends of the bags were pulled up to 1.5 m above the water surface thereby isolating the water in the mesocosms from the surrounding Baltic Sea.

To ensure a homogeneous water column in each mesocosm at the start of the experiment, the halocline present was destroyed by bubbling each mesocosm with compressed air for three and a half minutes on *t-5*. A video profile taken in one of the mesocosms on *t-4* shows the plankton community present at the beginning of the study period (Boxhammer et al., 2015). Figure 3 indicates the experiment timeline including important manipulations. Mesocosm bags were cleaned occasionally inside and outside throughout the experiment to minimise wall growth and keep the biofilm biomass at a minimum (see Fig. 3 and Riebesell et al. (2013) for further details). An isotope tracer (^{15}N-N_2 gas) specific to the nitrogen fixing organisms present was injected in two additions (*t22* and *t26*) to four mesocosm bags (M3, M5, M6, M8). Further details about the addition are described in Paul et al. (in preparation). No dissolved inorganic or organic nutrients were added to the mesocosms in this study. At the end of the experiment, the volume of each mesocosm (0 – 19 m) was determined through addition of a calibrated salt solution as described by Czerny et al. (2013). Final mesocosm volumes ranged between 53.1 and 55.1 m^3 with an estimated uncertainty of 2 %. Unfortunately three mesocosms (M2, M4 and M9) were lost because of extensive and unquantifiable water exchange with the surrounding seawater due to a welding error on the mesocosm bags, and were thus excluded from sampling and analyses.

2.2 CO_2 manipulations

CO_2 treatments were achieved by equally distributing filtered (50 µm), CO_2-saturated seawater into the mesocosm as described by Riebesell et al. (2013) in four separate additions (see Table 1 for details). The first addition of CO_2-enriched seawater defined the beginning of the experiment and took place on *t0* following sampling activities. Seawater for the additions was collected from 10 m depth by a pipe connected to the laboratory in the research station. Different amounts of CO_2-saturated seawater were added to four mesocosms to set-up an initial gradient in fCO_2 treatments from ambient (~240 µatm) up to ~1650 µatm. On *t15*, CO_2 was manipulated in the upper 7 m to counteract pronounced outgassing in the mesocosm. Two mesocosms were selected as controls with no addition of CO_2-enriched seawater. Instead unenriched filtered seawater (50 µm) was added for the initial manipulations. For the later smaller addition, the water distributor (‘spider’, Riebesell et al. (2013)) was pulled up and down in each mesocosm to simulate water column mixing and manipulation side effects caused by the device on *t15*.

2.3 CTD and light measurements

CTD casts in each mesocosm and in the surrounding water were made with a hand-held self-logging CTD probe (CTD60M, Sea and Sun Technology) from 0.3 m down to ~18 m (mesocosms) and to ~30 m (surrounding water in Archipelago = Baltic) between 13:30 and 14:30 local time (LT) daily until *t31*, and then every second day until *t46*. Temperature, pH, dissolved oxygen and PAR (photosynthetic active radiation) sensors were deployed on the CTD as well as a conductivity cell. Details on the sensors, their accuracy and precision and corrections applied are described in Schulz and Riebesell (2013). The potentiometric CTD pH was corrected to spectrophotometric measurements (see Section 2.5.1). The depth of average water column light intensity in metres was calculated by averaging all water column PAR data and relating this to the depth where this intensity of PAR occurred.

A PAR sensor (LICOR LI192) was placed unobstructed at the end of a 2 m pole on the roof of Tvärminne Zoological Station (~1 km from mesocosm mooring site) to record incoming PAR for the mesocosms. Incoming PAR was recorded from 14:43 LT, on 14 June 2012 continuously as the mean of integrated 60 second intervals until the end of the experiment at 11:23 LT on 7 August 2012.

2.4 Sampling procedures

Water samples were collected regularly from each mesocosm and the surrounding water using depth-integrated water samplers (IWS, HYDRO-BIOS Kiel). Unless otherwise reported, all samples are from the entire water column (0 to 17 m). For example, inorganic dissolved nutrient and fluorometric Chl *a* samples were also taken regularly for the upper water column (0 to 10 m). Full details of mesocosm sampling procedures and equipment are described in Riebesell et al. (2013) and Schulz et al. (2013). There were two intensive sampling periods where sampling took place every day (*t-3* to *t5*, *t29* to *t31*), otherwise most variables were sampled every second day. Table 2 presents sampled variables including sampling frequency and respective manuscripts which report each data set. Samples for carbonate chemistry variables and trace gas analyses were the first to be sampled and were taken from the IWS directly on board the sampling boat. Other samples (e.g. particulate matter, Chl *a*, phytoplankton pigments) were collected into 10 L carboys and stored in the dark. Carboys were stored at in situ temperature on-shore and sub-sampling from these carboys was usually within one hour and up to a maximum of five hours after sampling. Care was taken to mix the

water samples in the carboys well before taking subsamples to ensure homogeneous sampling for all parameters.

The sediment trap was emptied every second day using a manual vacuum pump system to acquire the settled material via a silicon tube reaching down to the collection cylinder of the sediment trap (Boxhammer et al., in prep., Riebesell et al., 2013). This material was used to quantify and characterise particle sinking flux. Subsamples of the particle suspension (<6 % in total) were taken before the material was concentrated. Particles and aggregates were allowed to settle down within two hours at in situ temperature before separation of the supernatant. Collected particulate material was then centrifuged, while subsamples of the supernatant were filtered and analysed analogous to water column samples for particulate matter. Centrifuged material was subsequently frozen, lyophilised and ground to a fine powder of homogeneous composition. From this powder small subsamples of between 0.7 and 1.5 mg were weighed and analysed for carbon, nitrogen, phosphate and biogenic silica content as described in this manuscript for water column samples (see section 2.5.3). Concentrations of particulate material were calculated based on total mesocosm volume (in L). Mesocosm volume determined on *t45* by salt addition in kg (Section 2.2) was converted using mean mesocosm temperature and salinity over 0 – 17 m between *t-3* and *t43* (mean temperature = 11.42 °C, mean salinity = 5.70) and the algorithms described by Fofonoff and Millard Jr. (1983). A more in-depth description of sampling and processing of particles collected in the sediment traps of the KOSMOS setup will be presented in Boxhammer et al. (in prep.).

2.5 Sample analyses

2.5.1 Carbonate system parameters (DIC, TA, pH_T)

Samples for total alkalinity (TA), dissolved inorganic carbon concentrations (DIC) and total pH (on the total pH scale: pH_T) were gently pressure-filtered (Sarstedt Filtropur PES, 0.2 µm pore size) using a membrane pump (Stepdos) to exclude calcareous particles and particulate organic material before analysis. Presence of particulate matter can influence precision of carbonate chemistry measurements. In addition, the sterile filtration eliminates the influence of biological processes on pH and DIC during sample storage by phytoplankton or bacteria.

Total pH was determined by spectrophotometry as described in Dickson et al. (2007). Samples were analysed on a Cary 100 (Varian) spectrophotometer in a temperature controlled

10 cm cuvette using a low ionic strength m-cresol indicator dye matching the salinity of the sample water and an appropriate low salinity pK (Mosley et al., 2004). CTD pH measurements were corrected to pH_T by daily linear correlations of mean water column potentiometric pH measurements to spectrophotometric pH_T measurements.

DIC concentrations were determined by infrared absorption using a LICOR LI-7000 on an AIRICA system (MARIANDA, Kiel). Measurements were made on four replicates of 2 mL sample volume and DIC was calculated as the mean of the best three out of four measurements. The precision was typically better than 1.5 µmol kg^{-1}. Dissolved calcium concentrations in seawater were determined by inductively coupled plasma optical emission spectroscopy (ICP-OES) using a VARIAN 720-ES and quality controlled with IAPSO reference material.

TA was analysed by potentiometric titration using a Metrohm 869 Sample Changer and a 907 Titrando Dosing unit according to the open cell method described in Dickson et al. (2007). Due to unaccounted contributions to TA in the range of 20 and 25 µmol kg^{-1} by components such as organic acids and bases, spectrophotometric pH_T and DIC were used to calculate carbonate chemistry speciation using the stoichiometric equilibrium constants for carbonic acid of Mehrbach et al. (1973) as refitted by Lueker et al. (2000). Buffering by organic compounds is not accounted for in the traditional TA definition (Dickson, 1981) and depends on unknown concentrations and acid/base equilibria of certain DOM components. Thus, using TA for carbonate chemistry speciation calculations would have resulted in errors (Koeve and Oschlies, 2012). Both TA and DIC measurements were calibrated using measurements of the certified reference material batch, CRM 115 (Dickson, 2010).

2.5.2 Dissolved inorganic nutrients

Samples for nutrients were collected in acid-cleaned (1 mol L^{-1} HCl) 60 mL low density polyethylene bottles (Nalgene), stored at 4°C in the dark following sampling and analysed within 12 hours of collection. Dissolved silicate (DSi) concentrations were determined using standard colorimetric techniques (Grasshoff et al., 1983) at the micromolar level using a nutrient autoanalyser (Seal Analytical, Quattro). Nanomolar levels of dissolved nitrate + nitrite (hereafter nitrate) and dissolved inorganic phosphate (DIP) were determined with a colorimetric method using a 2 m liquid waveguide capillary cell (LWCCs) (Patey et al., 2008; Zhang and Chi, 2002) with a miniaturised detector (Ocean Optics Ltd). Detection limits were 2 nmol L^{-1} for nitrate and 1 nmol L^{-1} for DIP, with a linear range up to

300 nmol L^{-1}. All samples for inorganic nutrient measurements were filtered using glass fibre filters (GF/F, nominal pore size of 0.7 µm, Fisher Scientific) prior to analysis. This was done to reduce the dissolution of nutrients from particulates during analysis, and also to avoid particles blocking the LWCCs and interfering with the spectrophotometric measurements. Ammonium (NH_4^+) measurements were undertaken following the method by Kérouel and Aminot (1997) with fluorimetric detection (Trilogy, Turner), and featuring a detection limit of 5 nmol L^{-1}.

2.5.3 Particulate material (C, N, P, Si)

Total particulate carbon, particulate organic nitrogen and total particulate phosphorus (TPC, PON, TPP) samples were collected onto combusted GF/F filters (Whatman, nominal pore size of 0.7 µm) using gentle vacuum filtration (<200 mbar) and stored in glass petri dishes at -20°C directly after filtration until analysis. Filters and glass petri dishes were combusted at 450°C for 6 hours before use. Filters were not acidified to distinguish between inorganic and organic particulate carbon before analyses hence we measured TPC. However, microscopy counts and total alkalinity drawdown indicated pelagic calcifying organisms were not abundant and there was no significant calcification, thus it was probably mostly particulate organic carbon. In addition to the total particulate matter fraction, gauze pre-filters were used to separate size-fractionated samples for C and N analyses (0.7 to 10 µm = $TPC/PON_{<10}$, 0.7 to 55 µm = $TPC/PON_{<55}$). Filtration volumes ranged from 500 mL for the total fraction (POM_{tot}) to up to 1500 mL for <55 µm size fraction to ensure sufficient biomass on the filter for analyses. Sampling for $TPC_{<10}$ and $PON_{<10}$ only occurred after isotope tracer addition on *t23* in the four mesocosms where tracer was added (M3, M5, M6, M8). This size fraction was sampled to exclude large filamentous diazotrophic cyanobacteria.

Filters for TPC/PON were dried at 60°C, packed into tin capsules and stored in a dessicator until analysis. TPC and PON measurements were made on an elemental analyser (EuroEA) according to Sharp (1974), coupled by either a Conflo II to a Finnigan Delta^{Plus} isotope ratio mass spectrometer or a Conflo III to a Thermo Finnigan Delta^{Plus} XP isotope ratio mass spectrometer. Sub-samples of sediment material powder (1 – 2 mg) were weighed directly into tin capsules using an electronic microbalance (Sartorius M2P) with an accuracy of 0.001 mg. In addition to the standard calibration at the beginning of each run, standard materials (caffeine, peptone, acetanilide, nicotinamide, glutamic acid) were also included within runs to identify any drift and ensure accuracy and full combustion of the samples during analysis.

Selected samples for sediment material TPC and PON were reanalysed on an elemental analyser (EuroEA) not coupled to a mass spectrometer using the same method and standard materials. Total sinking particle flux is the sum of both the particulate matter concentrations determined in sediment powder and supernatant.

Filters for total particulate phosphorus (TPP) were placed in 40 mL of deionised water (MilliQ, Millipore) with oxidising decomposition reagent (MERCK, Catalogue no. 112936) and autoclaved for 30 minutes in a pressure cooker to oxidise the organic phosphorus to orthophosphate. Samples were allowed to cool before concentrations were determined by spectrophotometric analysis as for dissolved inorganic phosphate concentrations according to Hansen and Koroleff (1999).

For biogenic silica (BSi), samples were collected on cellulose acetate filters (0.65 µm Whatman) as described above for TPC, PON and TPP. Particulate silicate was leached from filtered material using 0.1 mol L^{-1} NaOH at 85°C for 2 hours and 15 minutes, neutralised with H_2SO_4 (0.05 mol L^{-1}, Titrisol) and analysed as dissolved silicate by spectrophotometry according to Hansen and Koroleff (1999).

Content of TPP and BSi in finely ground sediment trap samples was determined from subsamples and analysed according to methods described for water column samples.

2.5.4 Dissolved organic matter (C, N, P)

For dissolved organic carbon (DOC) and total dissolved nitrogen (TDN) analyses, 35 mL of sample was filtered through pre-combusted GF/F filters (450°C, 6 h) and collected in acid cleaned and combusted glass vials (450°C, 6 h), acidified with HCl to pH 1.9 and then flame sealed, and dark-stored in a fridge (4°C) for subsequent analysis. DOC and TDN concentrations were determined using a high-temperature catalytic combustion technique with a Shimadzu TOC-TN V analyser following Badr et al. (2003). Acidified deep Sargasso Sea water, preserved in glass ampoules and provided by D. Hansell (University of Miami), served as a certified reference material. Our analytical precision, based on the coefficient of variation (standard deviation/mean) of consecutive measurements of a single sample (generally between 3 and 5 injections), was typically <1 %. Dissolved organic nitrogen (DON) concentrations were calculated from TDN by the subtraction of the inorganic nitrogen concentrations.

Dissolved organic phosphorus (DOP) samples were collected as for DOC and TDN but stored at -20°C in acid-rinsed, high density polyethylene (HDPE) bottles. Total dissolved phosphate was decomposed to inorganic phosphate using an oxidising solution and microwave radiation (MARS 5X microwave, CEM) before analysis according to Hansen and Koroleff (1983). DOP concentrations were calculated from total dissolved phosphate by subtracting dissolved inorganic phosphate concentrations. Samples for DOP were only taken until *t30*. For further details, please refer to Nausch et al. (in prep.).

2.5.5 Phytoplankton pigments

Samples for fluorometric chlorophyll *a* determination (Chl *a*) and for phytoplankton pigment analyses by reverse phase high performance liquid chromatography (HPLC) were collected as described for POM with care taken to minimise exposure to light. Size fractionation for HPLC samples was achieved by pre-filtration using a 20 µm mesh and 2 µm membrane filters (Nuclepore) and was sampling was undertaken every 4th day, except for between *t31* and *t39* where sampling occurred only on *t31*, *t33* and *t39* (Table 2). Filtration volume for the total and <2 µm fraction as well as for Chl *a* was 500 mL whereas for the large fraction (>20 µm) volume ranged between 3000 and 5000 mL. All HPLC samples were stored at -80°C for under 6 months and Chl *a* samples at -20°C overnight until analysis.

Pigments from both fluorometric and HPLC analyses were extracted in acetone (90 %) in plastic vials by homogenisation of the filters using glass beads in a cell mill. After centrifugation (10 min., 800 x g, 4°C) the supernatant was analysed on a fluorometer (TURNER 10-AU) to determine Chl *a* concentrations (Welschmeyer, 1994). Samples for phytoplankton pigment analyses were also centrifuged (10 min., 5200 rpm, 4°C) and the supernatant was filtered through 0.2 µm PTFE filters (VWR International). Phytoplankton pigment concentrations were determined in the supernatant by reverse phase high performance liquid chromatography (HPLC; WATERS HPLC with a Varian Microsorb-MV 100-3 C8 column (Barlow et al., 1997; Derenbach, 1969)) and peaks were calibrated with the help of a library of pre-measured commercial standards. Relative contributions of phytoplankton groups to total Chl *a* were calculated using the CHEMTAX matrix factorisation program (Mackey et al., 1996). Pigment ratios were adapted accordingly to those reported for Baltic Sea phytoplankton (Eker-Develi et al., 2008; Schluter et al., 2000; Zapata et al., 2000). The size fraction 2 – 20 µm was calculated as <2 µm and >20 µm subtracted from the total size fraction.

2.6 Statistical data treatment

As in previous mesocosm experiments, an fCO_2 gradient was chosen for reasons as outlined in Schulz et al. (2013). Linear regression analyses were used to determine the relationship between average fCO_2 and average response of the variables during each experimental phase. Outliers were detected based on Grubb's test ($p < 0.05$). This test was applied to all treatments by experiment phase to account for temporal development of each variable. Detected outliers were not included in the calculation of experiment phase average. Exceptions to outlier exclusion include a) biogenic silicate concentrations in M8 on *t23* because all data was higher on this particular sampling day, and b) C:N in total POM on *t19* in M8 because the C:N in this treatment was also markedly higher than other treatments on the following sampling day (*t21*) and c) the contribution of cryptophytes to total Chl *a* M8 on *t17* and d) all five outliers in contribution of euglenophytes to total Chl *a* detected in Phase III for the same line of reasoning as b). All data points are included in the figures with excluded outliers clearly marked. Linear regression analyses and outlier detection and exclusion were undertaken using R Project for Statistical Computing (http://www.r-project.org/).

3 Results

3.1 Variations in temperature, salinity and oceanographic conditions

Conditions in the Tvärminne Storfjärden at the beginning of the experiment and during mesocosm closure were typical for the early summer season. Daily solar irradiance was at the annual peak (summer solstice) and surface water temperatures were ~10°C. Daily average water column temperature was highly variable over the experiment ranging from 8.0 – 8.5°C at the beginning of the experiment to 16°C on *t16* (Fig. 4). Temperature variations as well as the first CO_2 manipulation on *t0* were used to define different experimental phases, (Phase 0 = *t-5* to *t0*, Phase I = *t1* to *t16*, Phase II = *t17* to *t30*, Phase III = *t31* to *t43*). Warming occurred over the first 15 days and average water column temperatures peaked at 16°C (Phase I). A cooling phase (Phase II) occurred until *t31* (~ 8°C), followed by a second warming period (Phase III) which continued until the end of the experiment reaching around 12°C on average in the water column (Fig. 4 and 5C). The cooling in Phase II occurred around the same time as a period of lower incoming PAR between *t15* and *t25* (land based PAR measurements, Fig. 6A). Surface water temperatures reached a maximum of 18°C with a surface-to-depth

gradient of 6°C. The water column in the mesocosms remained thermally stratified throughout the study according to daily CTD profiles. Stratification strength, defined here as the potential density anomaly (σ_T) difference between the surface 10 m and bottom 7 m above the sediment trap in each mesocosm, was variable but lower in Phase I than in II and III. Detected changes in density over time were largely driven by changes in temperature within the mesocosms as there was only a minimal increase in salinity during the experiment probably due to evaporation (Fig. 5). Here, M8 was arbitrarily selected as representative for all mesocosms in Figs. 5 and 6. A typical daily difference in measured average water column temperature and salinity between mesocosms was 0.04°C and 0.01, respectively. The increase in salinity on *t45* is from addition of a calibrated salt solution for mesocosm volume determination. A notable decrease in temperature and increase in salinity in the archipelago between *t15* and *t31* coincided with a period of stormy weather and a change in wind direction from north-easterly to a more westerly direction, indicating a period of upwelling. During this period, there was slightly lower incoming PAR indicating higher cloud cover (Fig. 6). The depth of average light intensity was relatively stable between 3.7 and 4.7 m inside the mesocosms and very similar between treatments over time (Fig. 6).

3.2 Temporal variations in carbonate system

All mesocosms had a similar pH_T of around 8.0 prior to CO_2 perturbations. Initial CO_2 enrichment reached target values on *t4* ranging from ~240 µatm in the two ambient control mesocosms up to ~1650 µatm in the highest treatment, corresponding to a pH_T range of ~7.45 to 8.2 (Fig. 7). Aside from the CO_2 addition on *t15*, fCO_2 was allowed to vary naturally and treatments remained well separated over the entire experiment. The decrease in fCO_2 over time in the high CO_2 treatment mesocosms was mostly driven by outgassing rather than biological uptake as productive biomass remained relatively low in this experiment (see section 3.3). The effect of outgassing is evident in the rapid increase in surface pH_T in all treatment mesocosms (Fig. 8). Surrounding water pH_T (0 – 17 m) ranged from 8.30 initially to 7.75 during the experiment. The profound pH_T variability outside the mesocosms was due to upwelling of deeper, CO_2-rich seawater. Within each mesocosm, CO_2 manipulations over the entire depth were relatively homogeneous initially. However a decrease in pH in the ambient control mesocosms below 5 m depth was detected from around *t15* onwards, suggesting heterotrophic activity at depth involving respiration of organic matter to CO_2 (Fig. 8). DIC increased in the control mesocosms due to gas exchange, which counteracted losses through

uptake by the plankton community which left the water column undersaturated in CO_2 compared to the overlying atmosphere (~230 µatm in control mesocosms vs. ~400 µatm in atmosphere (Schernewski, 2011)). Undersaturation of CO_2 is typical for post-spring bloom conditions such as those in the Tvärminne Storfjärden before the first CO_2 enrichment in this study on *t0*.

Calcium concentration was 2.17 mmol kg^{-1} which was higher than calculated from a typical mean ocean salinity relationship of 1.67 mmol kg^{-1} (Dickson et al., 2007), because of high riverine calcium carbonate inputs in the Baltic Sea (Feistel et al., 2010). We accounted for this in the calculation of the calcium carbonate saturation state in the water (Fig. 7D). All mesocosms apart from the two ambient controls during Phase 0 and I were undersaturated with respect to aragonite (Fig. 7D) and the highest three fCO_2 treatments were also undersaturated with respect to calcite (data not shown) during the entire experiment.

3.3 Effects of elevated CO_2

Out of 105 linear regressions applied to particulate and dissolved material from the water column and the accumulated sediment trap material to analyse the effect of CO_2, we detected a significant correlation in 18. These are summarised in Table 3 and highlighted in the following sections. The majority of detected responses (14) indicated a positive effect of CO_2 whereas only four indicated a negative effect of CO_2.

In this study, the low number of fCO_2 treatments (six) due to the exclusion of three mesocosms limited the statistical power of our conclusions. However the effect of CO_2 was consistent across biogeochemical element pools with higher sustained particulate matter concentrations and lower dissolved phosphate under high CO_2. This gives us confidence that the results of our study are indicative of the response of this particular plankton community in the Baltic Sea to ocean acidification.

3.4 Chlorophyll *a* dynamics

Chl *a* concentrations were low but typical of a post-spring bloom period. An increase in Chl *a* began after *t1* and signified a phase characterised by higher Chl *a* concentrations (~2 µg L^{-1}) until *t16* (Fig. 9, Phase I: *t1* to *t16*). Chl *a* concentrations decreased by ~0.8 µg L^{-1} in the mesocosms during Phase II and remained low and relatively stable in Phase III (~0.9 to 1.2 µg L^{-1}). Between 50 % and 80 % of Chl *a* was in the upper water column (IWS samples 0 – 10

m, Fig. 9C). Chl *a* concentrations were in general lower (0.9 to 2.5 µg L^{-1}) in the mesocosms than in the surrounding water (1.2 to 5.5 µg L^{-1}, Fig. 9). CO_2 related differences first developed during Phase II and remained stable during Phase III with 24 % higher Chl *a* in the highest fCO_2 treatment in Phase III (Table 3).

3.5 Dissolved inorganic and organic matter dynamics

No dissolved inorganic or organic nutrients were added to the mesocosms in this study and nutrient concentrations remained relatively stable with low inorganic nitrogen concentrations throughout the entire experiment. There was low inorganic nitrogen (~50 nmol L^{-1} nitrate and ~200 nmol L^{-1} ammonium) relative to phosphate (~150 nmol L^{-1}) in all mesocosms at the start of the study period compared to the canonical Redfield nutrient stoichiometry (Fig. 10, C:N:P = 106:16:1, Redfield (1958). These concentrations are within the natural range for this region in a post-spring/early summer bloom phase (Fig. 10). Fixed nitrogen availability primarily limited the development of phytoplankton biomass in this system. This is common in the Baltic Sea following the spring bloom (Matthäus et al., 1999). Temporal dynamics between phosphate and nitrate showed decoupling. Nitrate concentrations increased from ~20 nmol L^{-1} up to ~80 nmol L^{-1} from *t1* until the end of the experiment (*t43*), whereas phosphate concentrations were slightly more dynamic, decreasing in Phase I and increasing in Phases II and III (Fig. 11). Around *t30*, differences in phosphate concentrations between fCO_2 treatments became visible with a significant negative relationship between fCO_2 and phosphate concentration in Phase III (Table 3). For further details and discussion on phosphorus pool sizes, uptake rates and cycling, see Nausch et al. (in prep.).

Ammonium concentrations decreased from between ~170 and ~280 nmol L^{-1} on *t-3* to between 40 and 150 nmol L^{-1} on *t39* with a small increase until *t43* in all mesocosms (Fig 10C). Samples for NH_4^+ concentration were lost on *t27* and *t29* for all mesocosms. The strongest decrease occurred during Phase I and concentrations remained relatively stable in Phase II and III. No significant fCO_2 effect was detected during any experimental phase above the variability in the data. Inside the mesocosms, dissolved silicate concentrations decreased minimally from around 6.2 µmol L^{-1} on *t-1* to between 5.5 and 5.8 µmol L^{-1} at the end of the initial productive Phase I on *t16* (Fig. 10D). Thereafter, dissolved silicate remained relatively constant until the end of the experiment. No significant effect of fCO_2 on dissolved silicate concentrations was detected in any phase.

DOC concentrations ranged between 410 and 420 µmol L^{-1} on *t2* and increased by ~30 µmol L^{-1} up to between 440 and 450 µmol L^{-1} on *t43* (Fig. 11A). In Phase III, DOC positively correlated with fCO_2 (Table 3). There was no statistically significant correlation of fCO_2 with DON or DOP concentrations in any experimental phase. No clear temporal trends were distinguished in DOP concentrations although DON decreased during Phase I (Fig. 11). Where data points are missing, DON could not be corrected for NH_4^+ concentrations hence are excluded from the data set.

3.6 Particulate matter dynamics

Particulate C, N and P concentrations were higher in Phase I than in Phase II and III, (Fig. 12), as also observed for Chl *a* (Fig. 9A). The importance of small particles was even more pronounced in Phase III, where up to ~90 % of total particulate organic matter was attributed to the fraction $TPC_{<10}$ in the four mesocosms sampled for this size fraction (M3, M5, M6, M8, Fig. 12). In Phase III, there was a significant positive correlation between fCO_2 and average total TPC, PON and TPP (Table 3).

C:N and C:P ratios in POM_{tot} (Fig. 13) were above the Redfield ratio ($C:N:P_{tot}$ = 106:16:1) during the productive phase, peaked at the beginning of Phase I ($C:N_{tot}$ = 7 – 8.5, $C:P_{tot}$ = 110 - 160) then decreased and became stable during Phase II ($C:N_{tot}$ = 5.8 – 7.0, $C:P_{tot}$ = 80 - 140). Differences between fCO_2 treatments were first observed in Phase III with higher $C:N_{tot}$ in the highest fCO_2 treatment (Table 3). No significant effect of fCO_2 on N:P or C:P was detected in any experiment phase or in any size fraction.

BSi decreased from around 1.0 µmol L^{-1} at the beginning to ~0.3 µmol L^{-1} at the end of the experiment (Fig. 12). During Phase II, there was a statistically significant correlation of BSi with fCO_2, however this was absent in Phases I and III (Table 3).

3.7 Phytoplankton succession

The contribution to Chl *a* by different phytoplankton groups varied over time although the temporal trends in all mesocosms appeared remarkably similar (Fig. 14). Results from CHEMTAX analyses of the phytoplankton community present indicate that cryptophytes and chlorophytes had the highest contribution to total Chl *a* during Phase I and Phase II/III, respectively. The total abundances of cryptophytes decreased from *t-3* to *t17* in all mesocosms, succeeded by a brief euglenophyte peak around *t15*, with chlorophytes being the

dominant contributor to Chl *a* from *t17* on (Fig. 14). Total abundances of cyanobacteria, probably non-diazotrophic *Synechococcus*, were highest during both Phase II and III. Diatoms made up a relatively small proportion of the plankton assemblage and contributed to less than 10 % of Chl *a* in Phases I and II and between 10 – 25 % in Phase III. Other key groups detected included dinoflagellates and prasinophytes, however, they made up minor proportions (below 15% of total Chl *a*) of the plankton community throughout the entire experiment (dinoflagellate data not shown).

We analysed the relationship between fCO_2 and the contribution of phytoplankton groups to Chl *a* by linear regression for each experimental phase (Table 4). These analyses indicated small differences in plankton community composition between CO_2 treatments. There was a significant negative correlation between CO_2 and total diatom contribution to Chl *a* in Phase III. In Phase III, fCO_2 was also negatively correlated to the contribution of cryptophytes to Chl *a* and a significant positive effect on the contribution of prasinophytes to Chl *a*.

Linear regression of the absolute concentrations of a number of phytoplankton pigments in the size fraction <2 µm indicated primarily a positive correlation to fCO_2 during Phase I (i.e. Chl *a*, Violaxanthin, Neoxanthin) although a statistically significant effect was not detected in all pigments (Table 5). In Phase III, where the highest Chl *a* concentrations were in the size fraction <2 µm, mass balance calculations indicated more than 100% of total Chl *a* in this size range which is not physically possible. These unbalanced Chl *a* measurements are the result of measurement uncertainties at such low absolute concentrations, particularly in the >20 µm size fraction and of mass balance calculations between three independent filtrations. As the increase and decline in Chl *a* <2 µm and 2 – 20 µm fractions respectively are supported by flow cytometry data for picoeukaryote and nanoeukaryote abundances, we still consider the observed temporal variations to be robust. A positive correlation between picoeukaryote abundance and CO_2 treatment was also already detected in Phase I (Crawfurd et. al, in prep.). Absolute concentrations of Chl *a*, Chl *b*, Prasinoxanthin, Violaxanthin and Neoxanthin in the total fraction had a statistically significant positive correlation with fCO_2 during Phase III (see Table 5). Fucoxanthin concentrations (key pigment in diatoms but also present in dinoflagellates) and fCO_2 were also positively correlated in the fraction >20 µm during Phase III. Size fractionation of HPLC pigment analyses indicated a higher proportion of Chl *a* in all treatments in biomass <2 µm during Phases II and III (Fig. 15).

3.8 Sinking material flux

The amount of material collected in the sediment traps in each phase reflected biomass (here POM and Chl *a*) build-up from the water column. We calculated that >84 % of total carbon sinking into the sediment trap was collected during Phases I and II and less than 16 % during Phase III (Fig. 16). This corresponds to average accumulation rates (± standard deviation) of 0.303 ± 0.011, 0.203 ± 0.033 and 0.094 ± 0.029 µmol C L^{-1} day^{-1} across all mesocosms in Phases I, II and III respectively. No significant CO_2 trends were detected during any phase with regards to the total amount of C, N, P and BSi in the sediment trap material.

4 Discussion

4.1 Phase I: productive phase with high organic matter turnover

Phase I (*t1* to *t16*) was characterised by the highest sustained Chl *a* and particulate matter concentrations in the water column. Relatively high light availability, particularly between *t6* and *t15* (Fig. 6A), accompanied by increasing water column temperatures likely supported autotrophic growth. However, no increase in particulate matter pool size was observed in any treatment during this productive phase. Instead carbon was diverted into the sinking particle flux and DOC pool (Fig. 11) with a net daily accumulation of DOC of between 10 to 15 % of the total TPC pool between *t3* and *t13*. As inorganic nitrogen availability was very low, we assume this is due to carbon overconsumption (Toggweiler, 1993). Thus, organic matter turnover in the system appeared to be high during this period, although overall phytoplankton biomass production was limited by low inorganic nitrogen availability.

Although phytoplankton carbon fixation is expected to be stimulated by increased CO_2 availability (Hein and Sand-Jensen, 1997; Losh et al., 2012; Riebesell et al., 2007), previous CO_2 enrichment experiments using natural plankton assemblages under various conditions of nutrient repletion in different regions have shown no consistent response of primary production to elevated CO_2 (Engel et al., 2005; Hopkins et al., 2010; Hopkinson et al., 2010; Nielsen et al., 2011; Riebesell et al., 2007; Schulz et al., in prep.; Yoshimura et al., 2013). During high organic matter turnover in Phase I, we detected no statistically significant differences in bulk organic matter concentrations or elemental stoichiometry between CO_2 treatments. No effect CO_2 treatment could be detected in the most abundant, and presumably most productive, phytoplankton size class (2 – 20 µm, Fig. 15). Instead, detected differences between fCO_2 treatments in particulate matter in Phase I were mostly confined to pigment

concentrations in the smallest size fraction (<2 µm). Here, pigment concentrations were generally higher in the highest CO_2 treatment (Table 5). This is in line with flow cytometry counts which revealed a positive effect of CO_2 on the abundance of picoeukaryotes (Crawfurd et. al, in prep.) and is in agreement with studies in the Arctic (Brussaard et al., 2013), the sub-arctic North Pacific (Endo et al., 2013), and North Atlantic Ocean (Newbold et al., 2012) but contrasts the results from Richier et al. (2014) from shelf seas in the northeast Atlantic Ocean. The positive influence of CO_2 on phytoplankton pigment concentrations was also detected in the largest size fraction (>20 µm) in Phase I, however this size class made up only a small portion of total Chl *a* (<10 % Fig. 15, size fractionated pigment analyses). Thus, small CO_2-driven differences in plankton community structure in the smallest and largest phytoplankton were not relevant for biogeochemical element cycling in this plankton assemblage during this productive phase.

4.2 Phase II: decline in autotrophic biomass and organic matter turnover

The distinct changes in the phytoplankton communities in the mesocosms coincided with the decrease in temperature during the upwelling even in the Archipelago in Phase II (*t17* to *t30*). Temperature decreases of greater than 10°C in surface water, as observed in this study, have been reported for upwelling events during periods of thermal stratification (Lehmann and Myrberg, 2008) with considerable influence on the ecosystem productivity (Nômmann et al., 1991). Here we assume that the combination of higher grazing pressure, lower PAR and cooler temperatures likely slowed down phytoplankton productivity and contributed to decreased phytoplankton biomass, observed here as a decrease in Chl *a*, during this period (Fig. 9).

An increase in TPC_{tot}:Chl *a* from ~10 µmol μg^{-1} on *t17* to over 15 µmol μg^{-1} on *t29* indicates that carbon was being shifted from autotrophic to heterotrophic organisms, assuming that the Chl *a* content of the autotrophs remained constant. CTD profiles showed a decrease in pH_T below 10 m in both control mesocosms (Fig. 8) at the same time as surface Chl *a* (0 to 10 m) decreased between *t18* and *t30*. This pH decrease (i.e. CO_2 increase) could indicate a possible change in the equilibrium between dominance of autotrophic (CO_2 uptake) to heterotrophic (CO_2 release) processes during a phase of strong cooling in the lower water column. Higher organic material availability seemed to stimulate bacterial activity up until *t23* (Hornick et al., in prep.). Furthermore, higher zooplankton abundances after *t17* (Lischka et al., in prep.), as well as a peak in abundance of a potential mixotroph around *t17* (Euglenophycaea) also likely

contributed to higher organic matter remineralisation and CO_2 release. Hence Phase II is defined by increased heterotrophy and organic matter remineralisation. Carbon was primarily channelled into sinking material flux and higher trophic levels rather than accumulating in the DOC pool, mediated by increased zooplankton grazing pressure on primary producers.

Differences between CO_2 treatments in the dissolved and particulate matter pools developed during the Chl *a* decrease and apparent increase in net heterotrophy in Phase II. In addition, size-fractionated pigment analyses indicated a shift in phytoplankton community size to smaller organisms with up to ~90 % of Chl *a* in phytoplankton <2 µm at the end of Phase II. This was not caused by a remarkable gain in Chl *a* in the smaller size class but instead due to Chl *a* loss in the larger size class, which we think was driven by high grazing pressure from abundant zooplankton at this time (Lischka et al., in prep.). This removal of larger phytoplankton unmasked the underlying positive CO_2 response of picoplankton that was already present since Phase I but now became clearly visible. In other words, a positive CO_2 effect on picophytoplankton seemed to be present throughout the entire experiment. However, their ecological and biogeochemical relevance within the plankton community was too small initially, so that the CO_2 effect was not detectable in the other bulk biogeochemical element pools.

Interestingly, measured carbon fixation rates did not show any fertilising effect of CO_2 (Spilling et al., in prep.), whereas both respiration (Spilling et al., in prep.) and bacterial production rates between *t14* and *t23* (Hornick et al., in prep., Nausch et al., in prep.) were lower at higher CO_2. This suggests slower net particulate matter loss rather than increased production under ocean acidification (see Hornick et al. in prep. and Spilling et al. in prep. in this issue for more on this topic).

4.3 Phase III: inactive plankton community

While temperature increased again during Phase III, there did not seem to be any recovery of phytoplankton biomass to the same level as in Phase I. In Phase II autotrophic growth was apparently dampened so severely that it could not recover within the duration of this study and was likely strongly controlled by high zooplankton grazing pressure. There was very little change in the amount or stoichiometry of the particulate or dissolved matter pools suggesting that production and loss of particulate matter in the water column were either very low or relatively well balanced in Phase III. Only a small amount of TPC (~1 µmol L^{-1}, ~16% of

total suspended TPC) was collected in the sediment traps implying low particulate matter sinking flux strength in this phase. The positive (picoplankton-mediated) effect of CO_2 on particulate and dissolved pools unmasked in Phase II was sustained throughout Phase III in Chl *a*, TPC, PON, TPP and DIP. Thus in this study, higher autotrophic biomass was sustained under elevated CO_2 in this plankton community during the post-bloom phase and had a significant influence on biogeochemical pool sizes.

Variations in water column particulate matter concentrations did not translate into statistically significant differences in the amount of accumulated sediment trap material between CO_2 treatments. This may be because the response of CO_2 was the strongest in phytoplankton <2 µm, which taxonomically were likely to be chlorophytes and prasinophytes (Fig. 14B and 14F, Table 4). The unicellular organisms are, however, too small to sink as individual cells. Instead picoplankton contribute indirectly to carbon export through secondary processing of sinking picoplankton material (Richardson and Jackson, 2007). The positive effect of CO_2 on particulate matter pools was reflected positively in the DOC pool suggesting that a higher proportion of freshly produced organic matter was directed into the microbial food web, rather than being exported during the period of low organic matter turnover in Phase III. A similar channelling of carbon and the positive CO_2 response in the DOC pool was observed during nutrient-deplete conditions in an Arctic CO_2-enrichment mesocosm study (Engel et al., 2013). Here, this could be a consequence of continued reduced organic matter remineralisation at elevated CO_2 (Spilling et al., in prep.), as hypothesised for Phase II (see also section 4.2), although unfortunately no respiration data for Phase III is available.

Based on our results, we hypothesise that under future ocean acidification the Baltic Sea in low nitrogen, summer periods may shift towards a system where more organic matter is retained for longer time-periods in the upper water column but may not result in increased particulate matter sinking flux.

4.4 Potential ecosystem resilience under elevated CO_2

Although a significant, but small, response to CO_2 was detected in a number of particulate and dissolved matter pools, in numerous others no significant effect of CO_2 was detected in any phase (e.g. DON and DOP concentration, N:P and C:P in POM). The muted response of the plankton community and biogeochemistry to elevated CO_2 observed in this experiment might be linked to higher tolerance or resilience of the plankton community. The Baltic Sea is a

highly dynamic system with much larger annual temperature, light period, inorganic nutrient, pH, and salinity fluctuations than in many other major water bodies and the open ocean. Thus the community present in this study may have considerable physiological plasticity through exposure to large natural diurnal and annual fluctuations in carbonate chemistry speciation and pH (see also Joint et al. (2011) and Nielsen et al. (2011)). Low nitrogen availability in this study may have dampened underlying trends particularly in larger phytoplankton size classes. In past CO_2 enrichment experiments, nutrient addition amplified the existing effect of CO_2 between treatments, for example Schulz et al. (2013). This is one of few plankton community experiments, where nutrient concentrations were very low initially and concentrations and nutrient ratios were not manipulated. Such conditions are representative of a steady-state stratified water column present in many ecosystems for most of the year.

5 Conclusions

We observed higher post-bloom Chl *a*, particulate organic matter and DOC concentrations under elevated fCO_2 in this low nitrogen plankton community. No effect of CO_2 was identified in larger organisms (2 to 20 µm) which were dominant in the phytoplankton community during the period of higher productivity in Phase I. Hence their dominance masked the CO_2 signal from picophytoplankton in bulk particulate and dissolved pools. As a result of the shift in phytoplankton community size structure towards dominance of smaller phytoplankton size classes around three weeks after initial CO_2 enrichment, the underlying positive effect of CO_2 present on picophytoplankton (<2 µm) biomass since Phase I was revealed in particulate and dissolved matter pools. This signal could not be explained by a detectable increase in carbon fixation in this study (Spilling et al., in prep.).

Differences in water column biomass did not directly translate into increased particle sinking flux at higher fCO_2. Instead higher organic matter concentrations are more likely due to decreased net respiration at higher fCO_2 with the positive CO_2 effect on biomass channelled into the DOC pool. Alternatively secondary processing of sinking material may have removed the CO_2 signal present in the water column particulate matter, driven by picophytoplankton so that it was not reflected in the collected sinking material during the study period. Hence we suggest CO_2-induced changes in productivity in the upper water column may be decoupled from particle sinking flux.

In this study, it took almost four weeks until we first observed CO_2-related differences in the size and stoichiometry of some bulk biogeochemical pools. In many other variables, simulated ocean acidification did not have any significant effect at all. This slow response or lack of detected effect to ocean acidification may have been modulated by overall low inorganic nitrogen availability and high natural pH variability in the ecosystem. Therefore we recommend future experiments run for as long as practically feasible, focus on the vast oligotrophic regions and avoid nutrient additions. Changes in the abundance of key phytoplankton groups in steady-state systems due to higher CO_2 may underpin sustained fundamental changes in biogeochemical cycling in these regions.

Acknowledgements

We would like to thank Lidia Yebra and one anonymous referee for their constructive comments which improved the manuscript during the review process. We thank the KOSMOS team and all of the participants in the mesocosm campaign for their support during the experiment. In particular, we would like to thank Andrea Ludwig for co-ordinating the campaign logistics and assistance with CTD operations, the diving team, as well as Kerstin Nachtigall for analyses, and Josephine Goldstein, Mathias Haunost, Francois Legiret, Jana Meyer, Michael Meyerhöfer, and Jehane Ouriqua for assistance in sampling and analyses, Annegret Stuhr for helpful discussions, and Regina Surberg for calcium analyses. We would also like to sincerely thank the Tvärminne Zoological Station for their warm hospitality, support and use of facilities for this experiment. We also gratefully acknowledge the captain and crew of R/V ALKOR for their work transporting, deploying and recovering the mesocosms. This collaborative project was funded by Cluster of Excellence 'The Future Ocean' (Project CP1141) and by BMBF projects BIOACID II (FKZ 03F06550), SOPRAN Phase II (FKZ 03F0611), and the EU project, MESOAQUA (grant agreement number 228224).

References

Almén, A.-K., et al.: for submission for this Special Issue in Biogeosciences, in preparation

Badr, E.-S. A., Achterberg, E. P., Tappin, A. D., Hill, S. J. and Braungardt, C. B.: Determination of dissolved organic nitrogen in natural waters using high-temperature

catalytic oxidation, TrAC-Trend. Anal. Chem., 22(11), 819–827, doi:10.1016/S0165-9936(03)01202-0, 2003.

Barlow, R. G., Cummings, D. G. and Gibb, S. W.: Improved resolution of mono- and divinyl chlorophylls a and b and zeaxanthin and lutein in phytoplankton extracts using reverse phase C-8 HPLC, Mar. Ecol.-Prog. Ser., 161, 303–307, doi:10.3354/meps161303, 1997.

Biswas, H., Gadi, S. D., Ramana, V. V., Bharathi, M. D., Priyan, R. K., Manjari, D. T. and Kumar, M. D.: Enhanced abundance of tintinnids under elevated CO_2 level from coastal Bay of Bengal, Biodivers. Conserv., 21(5), 1309–1326, doi:10.1007/s10531-011-0209-7, 2012.

Boxhammer, T., Sswat, M., Paul, A. J., Nicolai, M., and Riebesell, U.: Video of a plankton community enclosed in a "Kiel Off-Shore Mesocosms for future Ocean Simulations" (KOSMOS) during a study in Tvärminne Storfjärden (Finland) 2012, doi:10.3289/KOSMOS_PLANKTON_FINLAND_2012, 2015.

Boxhammer, T., Bach, L. T., Czerny, J., and Riebesell, U.: Technical note: Sampling and processing of mesocosm sediment trap material for quantitative biogeochemical analysis, for submission for this Special Issue in Biogeosciences, in preparation.

Brussaard, C. P. D., Noordeloos, A. A. M., Witte, H., Collenteur, M. C. J., Schulz, K., Ludwig, A. and Riebesell, U.: Arctic microbial community dynamics influenced by elevated CO_2 levels, Biogeosciences, 10(2), 719–731, doi:10.5194/bg-10-719-2013, 2013.

Crawfurd, K., et al.: for submission for this Special Issue in Biogeosciences, in preparation.

Czerny, J., Schulz, K. G., Krug, S. A., Ludwig, A. and Riebesell, U.: Technical Note: The determination of enclosed water volume in large flexible-wall mesocosms "KOSMOS", Biogeosciences, 10(3), 1937–1941, doi:10.5194/bg-10-1937-2013, 2013.

Derenbach, J.: Zur Homogenisation des Phytoplanktons für die Chlorophyllbestimmung, Kieler Meeresforschungen, 25, 166–171, 1969.

Dickson, A. G.: An exact definition of total alkalinity and a procedure for the estimation of alkalinity and total inorganic carbon from titration data, Deep-Sea Res., 28(6), 609–623, 1981.

Dickson, A. G.: Standards for ocean measurements, Oceanography, 23(3), 34–47, doi:http://dx.doi.org/10.5670/oceanog.2010.22, 2010.

Dickson, A. G., Sabine, C. and Christian, J., Eds.: Guide to best practices for ocean CO_2 measurements, PICES Special Publication 3, 191 pp., http://aquaticcommons.org/1443/, 2007.

Doney, S. C., Mahowald, N., Lima, I., Feely, R. A., Mackenzie, F. T., Lamarque, J.-F. and Rasch, P. J.: Impact of anthropogenic atmospheric nitrogen and sulfur deposition on ocean acidification and the inorganic carbon system, P. Natl. Acad. Sci. USA, 104(37), 14580–14585, doi:10.1073/pnas.0702218104, 2007.

Dore, J. E., Lukas, R., Sadler, D. W., Church, M. J. and Karl, D. M.: Physical and biogeochemical modulation of ocean acidification in the central North Pacific, P. Natl. Acad. Sci. USA, 106(30), 12235–12240, doi:10.1073/pnas.0906044106, 2009.

Ekau, W., Auel, H., Pörtner, H.-O. and Gilbert, D.: Impacts of hypoxia on the structure and processes in pelagic communities (zooplankton, macro-invertebrates and fish), Biogeosciences, 7(5), 1669–1699, doi:10.5194/bg-7-1669-2010, 2010.

Eker-Develi, E., Berthon, J.-F. and Van der Linde, D.: Phytoplankton class determination by microscopic and HPLC-CHEMTAX analyses in the southern Baltic Sea, Mar. Ecol.-Prog. Ser., 359, 69–87, doi:10.3354/meps07319, 2008.

Endo, H., Yoshimura, T., Kataoka, T. and Suzuki, K.: Effects of CO_2 and iron availability on phytoplankton and eubacterial community compositions in the northwest subarctic Pacific, J. Exp. Mar. Biol. Ecol., 439, 160–175, doi:10.1016/j.jembe.2012.11.003, 2013.

Engel, A., Borchard, C., Piontek, J., Schulz, K. G., Riebesell, U. and Bellerby, R.: CO_2 increases ^{14}C primary production in an Arctic plankton community, Biogeosciences, 10(3), 1291–1308, doi:10.5194/bg-10-1291-2013, 2013.

Engel, A., Piontek, J., Grossart, H.-P., Riebesell, U., Schulz, K. G. and Sperling, M.: Impact of CO_2 enrichment on organic matter dynamics during nutrient induced coastal phytoplankton blooms, J. Plankton Res., 36(3), 641–657, doi:10.1093/plankt/fbt125, 2014.

Engel, A., Schulz, K. G., Riebesell, U., Bellerby, R., Delille, B. and Schartau, M.: Effects of CO_2 on particle size distribution and phytoplankton abundance during a mesocosm bloom experiment (PeECE II), Biogeosciences, 5(2), 509–521, doi:10.5194/bg-5-509-2008, 2008.

Engel, A., Zondervan, I., Aerts, K., Beaufort, L., Benthien, A., Chou, L., Delille, B., Gattuso, J.-P., Harlay, J. and Heemann, C.: Testing the direct effect of CO_2 concentration on a bloom

of the coccolithophorid *Emiliania huxleyi* in mesocosm experiments, Limnol. Oceanogr., 50(2), 493–507, doi:10.4319/lo.2005.50.2.0493, 2005.

Feistel, R., Weinreben, S., Wolf, H., Seitz, S., Spitzer, P., Adel, B., Nausch, G., Schneider, B. and Wright, D. G.: Density and absolute salinity of the Baltic Sea 2006–2009, Ocean Sci., 6(1), 3–24, doi:10.5194/os-6-3-2010, 2010.

Feng, Y., Hare, C. E., Rose, J. M., Handy, S. M., DiTullio, G. R., Lee, P. A., Smith Jr., W. O., Peloquin, J., Tozzi, S., Sun, J., Zhang, Y., Dunbar, R. B., Long, M. C., Sohst, B., Lohan, M. and Hutchins, D. A.: Interactive effects of iron, irradiance and CO_2 on Ross Sea phytoplankton, Deep-Sea Res. Pt. I, 57(3), 368–383, doi:10.1016/j.dsr.2009.10.013, 2010.

Fofonoff, N. P. and Millard Jr., R. C.: Algorithms for computation of fundamental properties of seawater, UNESCO Technical Papers in Marine Science, 44, pp. 56, 1983.

Gasiūnaitė, Z. R., Cardoso, A. C., Heiskanen, A.-S., Henriksen, P., Kauppila, P., Olenina, I., Pilkaitytė, R., Purina, I., Razinkovas, A., Sagert, S., Schubert, H. and Wasmund, N.: Seasonality of coastal phytoplankton in the Baltic Sea: Influence of salinity and eutrophication, Estuar. Coast. Shelf. S., 65(1–2), 239–252, doi:10.1016/j.ecss.2005.05.018, 2005.

Grasshoff, K., Ehrhardt, M., Kremling, K. and Almgren, T.: Methods of seawater analysis, Wiley Verlag Chemie GmbH, Weinheim, Germany, 1983.

Hama, T., Kawashima, S., Shimotori, K., Satoh, Y., Omori, Y., Wada, S., Adachi, T., Hasegawa, S., Midorikawa, T., Ishii, M., Saito, S., Sasano, D., Endo, H., Nakayama, T. and Inouye, I.: Effect of ocean acidification on coastal phytoplankton composition and accompanying organic nitrogen production, J. Oceanogr., 68(1), 183–194, doi:10.1007/s10872-011-0084-6, 2012.

Hansen, H. P. and Koroleff, F.: Determination of nutrients, in Methods of Seawater Analysis, edited by K. Grasshoff, K. Kremling, and M. Ehrhardt, pp. 159–228, Wiley Verlag Chemie GmbH, Weinheim, Germany, 1983.

Hansen, H. P. and Koroleff, F.: Determination of nutrients, in Methods of Seawater Analysis, edited by K. Grasshoff, K. Kremling, and M. Ehrhardt, pp. 159–228, Wiley Verlag Chemie GmbH, Weinheim, Germany, 1999.

Hare, C. E., Leblanc, K., DiTullio, G. R., Kudela, R. M., Zhang, Y., Lee, P. A., Riseman, S. and Hutchins, D. A.: Consequences of increased temperature and CO_2 for phytoplankton community structure in the Bering Sea, Mar. Ecol.-Prog. Ser., 352, 9–16, 2007.

Hein, M. and Sand-Jensen, K.: CO_2 increases oceanic primary production, Nature, 388(6642), 526–527, doi:10.1038/41457, 1997.

HELCOM: Climate change in the Baltic Sea Area: HELCOM thematic assessment in 2013, Helsinki Commission, Helsinki, Finland, 2013.

Hopkins, F. E., Turner, S. M., Nightingale, P. D., Steinke, M., Bakker, D. and Liss, P. S.: Ocean acidification and marine trace gas emissions, P. Natl. Acad. Sci. USA, 107(2), 760–765, doi:10.1073/pnas.0907163107, 2010.

Hopkinson, B. M., Xu, Y., Shi, D., McGinn, P. J. and Morel, F. M. M.: The effect of CO_2 on the photosynthetic physiology of phytoplankton in the Gulf of Alaska, Limnol. Oceanogr., 55(5), 2011–2024, doi:10.4319/lo.2010.55.5.2011, 2010.

Hoppe, C. J. M., Hassler, C. S., Payne, C. D., Tortell, P. D., Rost, B. and Trimborn, S.: Iron limitation modulates ocean acidification effects on Southern Ocean phytoplankton communities, PLoS ONE, 8(11), e79890, doi:10.1371/journal.pone.0079890, 2013.

Hornick, T., et al.: for submission for this Special Issue in Biogeosciences, in preparation.

Joint, I., Doney, S. and Karl, D.: Will ocean acidification affect marine microbes?, ISME J., 5(1), 1–7, doi:10.1038/ismej.2010.79, 2011.

Kanoshina, I., Lips, U. and Leppänen, J.-M.: The influence of weather conditions (temperature and wind) on cyanobacterial bloom development in the Gulf of Finland (Baltic Sea), Harmful Algae, 2(1), 29–41, doi:10.1016/S1568-9883(02)00085-9, 2003.

Kérouel, R. and Aminot, A.: Fluorometric determination of ammonia in sea and estuarine waters by direct segmented flow analysis, Mar. Chem., 57(3–4), 265–275, doi:10.1016/S0304-4203(97)00040-6, 1997.

Kim, J.-M., Lee, K., Shin, K., Kang, J.-H., Lee, H.-W., Kim, M., Jang, P.-G. and Jang, M.-C.: The effect of seawater CO_2 concentration on growth of a natural phytoplankton assemblage in a controlled mesocosm experiment, Limnol. Oceanogr., 51(4), 1629–1636, 2006.

Koeve, W. and Oschlies, A.: Potential impact of DOM accumulation on fCO_2 and carbonate ion computations in ocean acidification experiments, Biogeosciences, 9(10), 3787–3798, doi:10.5194/bg-9-3787-2012, 2012.

Law, C. S., Breitbarth, E., Hoffmann, L. J., McGraw, C. M., Langlois, R. J., LaRoche, J., Marriner, A. and Safi, K. A.: No stimulation of nitrogen fixation by non-filamentous diazotrophs under elevated CO_2 in the South Pacific, Glob. Change Biol., 18(10), 3004–3014, doi:10.1111/j.1365-2486.2012.02777.x, 2012.

Lehmann, A. and Myrberg, K.: Upwelling in the Baltic Sea — A review, J. Marine Syst., 74, S3–S12, doi:10.1016/j.jmarsys.2008.02.010, 2008.

Lischka, S., et al.: Micro- and mesozooplankton community response to increasing levels of CO_2 in the Baltic Sea: insights from a large-scale mesocosm experiment, for submission for this Special Issue in Biogeosciences, in preparation.

Lomas, M. W., Hopkinson, B. M., Ryan, J. L. L. D. E., Shi, D. L., Xu, Y. and Morel, F. M. M.: Effect of ocean acidification on cyanobacteria in the subtropical North Atlantic, Aquat. Microb. Ecol., 66(3), 211–222, doi:10.3354/ame01576, 2012.

Losh, J. L., Morel, F. M. M. and Hopkinson, B. M.: Modest increase in the C:N ratio of N-limited phytoplankton in the California Current in response to high CO_2, Mar. Ecol.-Prog. Ser., 468, 31–42, doi:10.3354/meps09981, 2012.

Lueker, T. J., Dickson, A. G. and Keeling, C. D.: Ocean pCO_2 calculated from dissolved inorganic carbon, alkalinity, and equations for K1 and K2: validation based on laboratory measurements of CO_2 in gas and seawater at equilibrium, Mar. Chem., 70(1–3), 105–119, doi:10.1016/S0304-4203(00)00022-0, 2000.

Mackey, M. D., Mackey, D. J., Higgins, H. W. and Wright, S. W.: CHEMTAX - A program for estimating class abundances from chemical markers: Application to HPLC measurements of phytoplankton, Mar. Ecol.-Prog. Ser., 144(1-3), 265–283, doi:10.3354/meps144265, 1996.

Matthäus, W., Nausch, G., Lass, H. U., Nagel, K. and Siegel, H.: The Baltic Sea in 1998 — characteristic features of the current stagnation period, nutrient conditions in the surface layer and exceptionally high deep water temperatures, Deutsche Hydrographische Zeitschrift, 51(1), 67–84, doi:10.1007/BF02763957, 1999.

Mehrbach, C., Culberson, C. H., Hawley, J. E. and Pytkowicz, R. M.: Measurement of apparent dissociation constants of carbonic acid in seawater at atmospheric pressure, Limnol. Oceanogr., 18(6), 897–907, 1973.

Meier, H. E. M., Andersson, H. C., Eilola, K., Gustafsson, B. G., Kuznetsov, I., Müller-Karulis, B., Neumann, T. and Savchuk, O. P.: Hypoxia in future climates: A model ensemble study for the Baltic Sea, Geophys. Res. Lett., 38(24), L24608, doi:10.1029/2011GL049929, 2011.

Mosley, L. M., Husheer, S. L. G. and Hunter, K. A.: Spectrophotometric pH measurement in estuaries using thymol blue and m-cresol purple, Mar. Chem., 91(1–4), 175–186, doi:10.1016/j.marchem.2004.06.008, 2004.

Nausch, M., et al.: for submission for this Special Issue in Biogeosciences, in preparation.

Newbold, L. K., Oliver, A. E., Booth, T., Tiwari, B., DeSantis, T., Maguire, M., Andersen, G., Van der Gast, C. J. and Whiteley, A. S.: The response of marine picoplankton to ocean acidification, Environ. Microbiol., 14(9), 2293–2307, doi:10.1111/j.1462-2920.2012.02762.x, 2012.

Nielsen, L. T., Hallegraeff, G. M., Wright, S. W. and Hansen, P. J.: Effects of experimental seawater acidification on an estuarine plankton community, Aquat. Microb. Ecol., 65(3), 271–285, doi:10.3354/ame01554, 2011.

Nielsen, L. T., Jakobsen, H. H. and Hansen, P. J.: High resilience of two coastal plankton communities to twenty-first century seawater acidification: Evidence from microcosm studies, Mar. Biol. Res., 6(6), 542–555, doi:10.1080/17451000903476941, 2010.

Nômmann, S., Sildam, J., Nôges, T. and Kahru, M.: Plankton distribution during a coastal upwelling event off Hiiumaa, Baltic Sea: impact of short-term flow field variability, Cont. Shelf Res., 11(1), 95–108, doi:10.1016/0278-4343(91)90037-7, 1991.

Patey, M. D., Rijkenberg, M. J. A., Statham, P. J., Stinchcombe, M. C., Achterberg, E. P. and Mowlem, M.: Determination of nitrate and phosphate in seawater at nanomolar concentrations, TrAC-Trend. Anal. Chem., 27(2), 169–182, doi:10.1016/j.trac.2007.12.006, 2008.

Paul, A. J., Achterberg, E. P., Bach, L. T., Boxhammer, T., Czerny, J., Haunost, M., Schulz, K.-G., Stuhr, A. and Riebesell, U.: No measureable effect of ocean acidification on nitrogen

biogeochemistry in a Baltic Sea plankton community, for submission for this Special Issue in Biogeosciences, in preparation.

Redfield, A. C.: The biological control of chemical factors in the environment, Am. Scientist, 46(3), 205–221, 1958.

Richardson, T. L. and Jackson, G. A.: Small phytoplankton and carbon export from the surface ocean, Science, 315(5813), 838–840, doi:10.1126/science.1133471, 2007.

Richier, S., Achterberg, E. P., Dumousseaud, C., Poulton, A. J., Suggett, D. J., Tyrrell, T., Zubkov, M. V. and Moore, C. M.: Phytoplankton responses and associated carbon cycling during shipboard carbonate chemistry manipulation experiments conducted around Northwest European shelf seas, Biogeosciences, 11(17), 4733–4752, doi:10.5194/bg-11-4733-2014, 2014.

Riebesell, U., Czerny, J., Von Bröckel, K., Boxhammer, T., Büdenbender, J., Deckelnick, M., Fischer, M., Hoffmann, D., Krug, S. A., Lentz, U., Ludwig, A., Muche, R. and Schulz, K. G.: Technical Note: A mobile sea-going mesocosm system – new opportunities for ocean change research, Biogeosciences, 10(3), 1835–1847, doi:10.5194/bg-10-1835-2013, 2013.

Riebesell, U., Schulz, K. G., Bellerby, R. G. J., Botros, M., Fritsche, P., Meyerhöfer, M., Neill, C., Nondal, G., Oschlies, A., Wohlers, J. and Zöllner, E.: Enhanced biological carbon consumption in a high CO_2 ocean, Nature, 450(7169), 545–548, doi:10.1038/nature06267, 2007.

Riebesell, U. and Tortell, P. D.: Effects of ocean acidification on pelagic organisms and ecosystems, in Ocean Acidification, edited by J.-P. Gattuso and L. Hansson, p. 99, Oxford University Press., 2011.

Rossoll, D., Sommer, U. and Winder, M.: Community interactions dampen acidification effects in a coastal plankton system, Mar. Ecol.-Prog. Ser., 486, 37–46, doi:10.3354/meps10352, 2013.

Rost, B., Zondervan, I. and Wolf-Gladrow, D.: Sensitivity of phytoplankton to future changes in ocean carbonate chemistry: current knowledge, contradictions and research directions, Mar. Ecol.-Prog. Ser., 373, 227–237, doi:10.3354/meps07776, 2008.

Schernewski, G.: Global Change and Baltic Coastal Zones, Springer Science & Business Media., 2011.

Schluter, L., Mohlenberg, F., Havskum, H. and Larsen, S.: The use of phytoplankton pigments for identifying and quantifying phytoplankton groups in coastal areas: testing the influence of light and nutrients on pigment/chlorophyll a ratios, Mar. Ecol.-Prog. Ser., 192, 49–63, doi:10.3354/meps192049, 2000.

Schulz, K. G., et al.: in prep.

Schulz, K. G., Bellerby, R. G. J., Brussaard, C. P. D., Büdenbender, J., Czerny, J., Engel, A., Fischer, M., Koch-Klavsen, S., Krug, S. A., Lischka, S., Ludwig, A., Meyerhöfer, M., Nondal, G., Silyakova, A., Stuhr, A. and Riebesell, U.: Temporal biomass dynamics of an Arctic plankton bloom in response to increasing levels of atmospheric carbon dioxide, Biogeosciences, 10(1), 161–180, doi:10.5194/bg-10-161-2013, 2013.

Schulz, K. G. and Riebesell, U.: Diurnal changes in seawater carbonate chemistry speciation at increasing atmospheric carbon dioxide, Mar. Biol., 160(8), 1889–1899, doi:10.1007/s00227-012-1965-y, 2013.

Schulz, K. G., Riebesell, U., Bellerby, R. G. J., Biswas, H., Meyerhöfer, M., Müller, M. N., Egge, J. K., Nejstgaard, J. C., Neill, C., Wohlers, J. and Zöllner, E.: Build-up and decline of organic matter during PeECE III, Biogeosciences, 5(3), 707–718, doi:10.5194/bg-5-707-2008, 2008.

Sharp, J.: Improved analysis for particulate organic carbon and nitrogen from seawater, Limnol. Oceanogr., 19(6), 984–989, 1974.

Spilling, K., et al.: for submission for this Special Issue in Biogeosciences, in preparation.

Stal, L. J., Staal, M. and Villbrandt, M.: Nutrient control of cyanobacterial blooms in the Baltic Sea, Aquatic Microbial Ecology, 18(2), 165–173, doi:doi:10.3354/ame018165, 1999.

Suikkanen, S., Pulina, S., Engström-Öst, J., Lehtiniemi, M., Lehtinen, S. and Brutemark, A.: Climate change and eutrophication induced shifts in northern summer plankton communities, PLoS ONE, 8(6), e66475, doi:10.1371/journal.pone.0066475, 2013.

Sutton, M. A., Howard, C. M., Erisman, J. W., Billen, G., Bleeker, A., Grennfelt, P., Grinsven, H. van and Grizzetti, B.: The European Nitrogen Assessment: Sources, Effects and Policy Perspectives, Cambridge University Press., 2011.

Tatters, A. O., Roleda, M. Y., Schnetzer, A., Fu, F., Hurd, C. L., Boyd, P. W., Caron, D. A., Lie, A. A. Y., Hoffmann, L. J. and Hutchins, D. A.: Short- and long-term conditioning of a

temperate marine diatom community to acidification and warming, Philos. T. Roy. Soc. B, 368(1627), 20120437, doi:10.1098/rstb.2012.0437, 2013a.

Tatters, A. O., Schnetzer, A., Fu, F., Lie, A. Y. A., Caron, D. A. and Hutchins, D. A.: Short- versus long-term responses to changing CO_2 in a coastal dinoflagellate bloom: Implications for interspecific competitive interactions and community structure, Evolution, 67(7), 1879–1891, doi:10.1111/evo.12029, 2013b.

The International Council for the Exploration of the Sea: ICES Dataset on Ocean Hydrography., ICES Oceanography Baltic Sea Monitoring Data [online] Available from: http://ocean.ices.dk/helcom/Helcom.aspx?Mode=1 (Accessed 7 August 2014), 2014.

Toggweiler, J. R.: Carbon overconsumption, Nature, 363(6426), 210–211, doi:10.1038/363210a0, 1993.

Turner, R. E.: Some Effects of Eutrophication on Pelagic and Demersal Marine Food Webs, in Coastal Hypoxia: Consequences for Living Resources and Ecosystems, edited by N. N. Rabalais and R. E. Turner, pp. 371–398, American Geophysical Union., 2001.

Vehmaa, A., et al.: for submission for this Special Issue in Biogeosciences, in preparation

Welschmeyer, N. A.: Fluorometric analysis of chlorophyll a in the presence of chlorophyll b and pheopigments, Limnol. Oceanogr., 39(8), 1985–1992, doi:10.4319/lo.1994.39.8.1985, 1994.

Wu, R. S. S.: Hypoxia: from molecular responses to ecosystem responses, Mar. Pollut. Bull., 45(1–12), 35–45, doi:10.1016/S0025-326X(02)00061-9, 2002.

Yoshimura, T., Nishioka, J., Suzuki, K., Hattori, H., Kiyosawa, H. and Watanabe, Y. W.: Impacts of elevated CO_2 on organic carbon dynamics in nutrient depleted Okhotsk Sea surface waters, J. Exp. Mar. Biol. Ecol., 395(1–2), 191–198, doi:10.1016/j.jembe.2010.09.001, 2010.

Yoshimura, T., Sugie, K., Endo, H., Suzuki, K., Nishioka, J. and Ono, T.: Organic matter production response to CO_2 increase in open subarctic plankton communities: Comparison of six microcosm experiments under iron-limited and -enriched bloom conditions, Deep-Sea Res. Pt I, 94, 1–14, doi:10.1016/j.dsr.2014.08.004, 2014.

Yoshimura, T., Suzuki, K., Kiyosawa, H., Ono, T., Hattori, H., Kuma, K. and Nishioka, J.: Impacts of elevated CO_2 on particulate and dissolved organic matter production: microcosm

experiments using iron-deficient plankton communities in open subarctic waters, J. Oceanogr., 69(5), 601–618, doi:10.1007/s10872-013-0196-2, 2013.

Zapata, M., Rodriguez, F. and Garrido, J. L.: Separation of chlorophylls and carotenoids from marine phytoplankton: a new HPLC method using a reversed phase C-8 column and pyridine-containing mobile phases, Mar. Ecol.-Prog. Ser., 195, 29–45, doi:10.3354/meps195029, 2000.

Zhang, J.-Z. and Chi, J.: Automated analysis of nanomolar concentrations of phosphate in natural waters with liquid waveguide, Environ. Sci. Technol., 36(5), 1048–1053, doi:10.1021/es011094v, 2002.

Tables and figures

Table 1. Volumes of CO_2-enriched seawater added for the CO_2 manipulation indicating day of addition and total manipulation volumes. Symbols and colours indicated here indicated here are used in all following figures.

Mesocosm		**M1**	**M5**	**M7**	**M6**	**M3**	**M8**	**Baltic**
Target fCO_2 (µatm)		ambient/ control	ambient/ control	600	950	1300	1650	ambient
Average fCO_2 (µatm) *t1 – t43*		365	368	497	821	1007	1231	417
Average fCO_2 (µatm) *t1 – t30*		346	348	494	868	1075	1333	343
Symbol								
Day	*t0*	-	-	20 L	50 L	65 L	75 L	-
	t1	-	-	10 L	40 L	50 L	65 L	-
	t2	-	-	10 L	30 L	45 L	50 L	-
	t3	-	-	5 L	8 L	9 L	10 L	-
	t15	-	-	-	9 L	12 L	18 L	-
	Total	-	-	45 L	137 L	181 L	218 L	-

Table 2. Summary of sampled variables for this study, including a brief description of method used, sampling frequency and corresponding manuscript in this Special Issue where data set and further details of methods used can be found.

Variable	Method/Instrument	Sampling frequency	Corresponding manuscript
ATP and phosphate uptake rates	^{33}P incorporation	Every 2nd day until *t29*	Nausch et al. in prep.
Bacteria and virus abundances	Flow cytometry	Daily until *t31*, then every 2nd day until *t43*	Crawfurd et al. in prep.
Bacterial production	^{14}C-Leucine incorporation	*t-3, t0,* from *t2* every 3rd day until *t26,* from *t29* every 2nd day until *t43*	Hornick et al., Nausch et al. in prep
Biogenic silica	Spectrophotometry	Every 2nd day until *t43*	This manuscript
Chlorophyll *a*	Fluorometry	Daily until *t30*, every 2nd day until *t39*	This manuscript
Community respiration	O_2 consumption	Daily until *t33*, excluding *t2*, *t14*, *t32*	Spilling et al. in prep.
Copepod (*Acartia bifilosa*, *Eurytemora affinis*) reproduction	Incubations, microscopy counts	Weekly *(t3, t10, t17, t24 + t45 for A. bifilosa)*	Almén et al. in prep, Vehmaa et al. in prep.
Copepod adult female size (*A. bifilosa*)	Microscopy measurements	Weekly (*t3*, *t10*, *t17*, *t24*, *t45*)	Vehmaa et al. in prep.
Copepod antioxidant capacity	ORAC	Weekly (*t3*, *t10*, *t17*,*t31*)	Almén et al. in prep, Vehmaa et al. in prep.
Dissolved inorganic carbon (DIC)	IR absorption	Daily until *t30*, every 2nd day until *t43*	This manuscript
Dissolved organic carbon and nitrogen	Shidmadzu TOC/TDN analyser	Every 2nd day until *t43*	This manuscript
Dissolve organic phosphorus	Microwave digestion, spectrophotometry	Every 2nd day until *t29*	This manuscript, Nausch et al. in prep.
Fatty acid concentrations (phytoplankton, copepods: *A.bifilosa*, *E.affinis*)	GC-MS	Phyto.: every 4th day until *t29*, Copepods: weekly (*t3*, *t10*, *t17*, *t24*, *t31*, *t38*)	Almén et al. in prep, Bermudez et al. in prep.
Fatty acid concentrations (*E.affinis* adults and eggs from reproduction incubations)	GC-MS	Weekly (*t7*, *t14*, *t21*, *t28*)	Almén et al. in prep
Inorganic nutrient concentrations	Colorimetry (LWCC)	Every 2nd day until *t43*	This manuscript
Light intensity (PAR)	LICOR sensor	Daily between *t-5* and *t45*	This manuscript
Mesozooplankton abundances	Stereomicroscopy counts	*t-3, t-2, t-1, t0, t3, t10, t17, t24, t31, t38, t43*	Lischka et al. in prep.
Microzooplankton abundances	Microscopy counts	*t-3, t0,t2, t4, t7,t9, t11, t13, t15,t17, t21, t23, t25, t27, t29, t31, t33, t35, t37, t39, t41, t43*	Lischka et al. in prep.
N_2-fixation rates	^{15}N incorporation, EA-IRMS	Every 2nd day until *t43*	Paul et al. in prep.
pH	Spectrophotometry and CTD sensor for mesocosm profiles	Daily until *t30*, every 2nd day until *t43*	This manuscript
Phytoplankton abundances	Microscopy counts	Every 2nd day until *t43*	Bermudez et al. in prep, Paul et al. in prep.
Phytoplankton abundances	Flow cytometry	Daily until *t31*, then every 2nd day until *t39*	Crawfurd et al. in prep
Phytoplankton pigments	HPLC	Every 2nd day until *t43*, size fractions every 2nd sampling day excluding *t37* and *t39*	This manuscript
Primary production	^{14}C incorporation	Every 2nd day until *t30*, excluding *t1*, *t2*, *t3*, *t6*, *t7*, *t8*	Spilling et al. in prep.
Salinity, Temperature	CTD sensor	Daily until *t30*, every 2nd day until *t43*	This manuscript
Sediment trap material – amount and elemental characterization (C,N, P, BSi, pigment concentration)	EA-IRMS, HPLC, spectrophotometry	Every 2nd day until *t43*	This manuscript, Paul et al. in prep.
Total alkalinity	Potentiometric titration	Daily until *t30*, every 2nd day until *t43*	This manuscript
Total particulate carbon (including δ^{13}C), particulate organic nitrogen (including δ^{15}N), size fractions (total, <55 µm, <10 µm)	EA-IRMS	Every 2nd day until *t43*,except for <10 µm fraction every 2nd day from *t23* until *t43*	This manuscript, Paul et al. in prep. (δ^{13}C unpublished)
Total particulate phosphorus	Spectrophotometry	Every 2nd day until *t43*	This manuscript
Trace gas concentration	GC-MS	Every 2nd day until *t17* then daily until *t30*	Webb et al. in prep.
Viral lysis and grazing of bacteria	Incubations, Flow cytometry	*t-3, t0, t4, t7, t11, t14, t18, t21*	Crawfurd et al. in prep
Viral lysis and grazing of phytoplankton	Incubations, Flow cytometry	*t1, t3, t6, t10, t13, t17, t20, t24, t31*	Crawfurd et al. in prep

Table 3. Summary of linear regression analyses of CO_2 effects on particulate and dissolved matter and sediment trap material including elemental stoichiometry in different size fractions for each experimental phase. fCO_2 and the parameter were averaged for each phase and using a linear model, a regression analysis was done to test for statistical significance of a potential CO_2 effect. Significant positive effects detected are in bold, significant negative effects of CO_2 are in italics. Degrees of freedom = 4, apart from particulate matter size fraction <10 µm where n = 2.

	Particulate matter				**Dissolved matter and Chl *a***				**Sediment material**			
	Parameter	*p*	Multiple R^2	F-statistic	Parameter	*p*	Multiple R^2	F-statistic	Parameter	*p*	Multiple R^2	F-statistic
Phase I	TPC total	0.152	0.438	3.113	Nitrate (0 – 17 m)	0.547	0.098	0.433	Total accumulated material	0.265	0.296	1.680
Phase II		0.902	0.761	12.760		0.602	0.074	0.320		0.593	0.078	0.336
Phase III		**0.011**	**0.834**	**20.070**		0.768	0.034	0.105		0.945	0.001	0.005
Phase I	TPC < 55 µm	0.580	0.083	0.363	Nitrate (0 – 10 m)	0.709	0.085	0.185	Total accumulated material in phase	0.265	0.296	1.680
Phase II		0.536	0.103	0.458		*0.033*	*0.718*	*10.170*		0.799	0.018	0.074
Phase III		0.759	0.026	0.108		0.540	0.101	0.448		0.372	0.202	1.010
Phase I	TPC < 10 µm	--	--	--	DIP (0 – 17 m)	0.486	0.128	0.589	Cumulative TPC in phase	0.752	0.028	0.115
Phase II		**0.036**	**0.929**	**26.120**		0.076	0.587	5.679		0.902	0.004	0.017
Phase III		0.187	0.661	3.899		*0.003*	*0.910*	*40.170*		0.386	0.191	0.947
Phase I	PON total	0.668	0.051	0.214	DIP (0 – 10 m)	0.651	0.056	0.239	Cumulative PON in phase	0.848	0.010	0.042
Phase II		0.490	0.126	0.576		0.075	0.589	5.737		0.662	0.052	0.222
Phase III		**0.001**	**0.940**	**62.890**		*0.030*	*0.732*	*10.950*		0.309	0.253	1.357
Phase I	PON < 55 µm	0.640	0.060	0.255	NH_4^+ (0 – 17 m)	0.225	0.340	2.058	Cumulative TPP in phase	0.621	0.067	0.286
Phase II		0.516	0.113	0.508		0.297	0.265	1.439		0.749	0.028	0.117
Phase III		0.381	0.195	0.968		0.217	0.349	2.147		0.358	0.212	1.079
Phase I	PON < 10 µm	--	--	--	Dissolved silicate	0.389	0.189	0.930	Cumulative BSi in phase	0.950	0.001	0.005
Phase II		0.207	0.630	3.401		0.272	0.288	1.617		0.850	0.010	0.041
Phase III		0.098	0.813	8.703		0.642	0.059	0.252		0.108	0.515	4.255
Phase I	TPP	0.084	0.567	5.240	P*	0.554	0.094	0.416				
Phase II		0.363	0.208	1.050		0.549	0.096	0.427				
Phase III		**0.004**	**0.897**	**34.690**		*0.003*	*0.918*	*44.470*				
Phase I	Biogenic silica (BSi)	0.070	0.601	6.032	DOC	0.324	0.240	1.262				
Phase II		**0.034**	**0.717**	**10.120**		0.230	0.334	2.006				
Phase III		0.553	0.095	0.419		**0.005**	**0.882**	**29.920**				
Phase I	C:N in total POM	0.653	0.056	0.236	DON	0.652	0.056	0.236				
Phase II		**0.020**	**0.779**	**14.080**		0.358	0.212	1.079				
Phase III		**0.050**	**0.659**	**7.716**		0.926	0.002	0.010				
Phase I	C:N in POM < 55 µm	0.487	0.128	0.587	DOP	0.914	0.003	0.013				
Phase II		0.208	0.360	2.249		0.391	0.188	0.924				
Phase III		**0.037**	**0.704**	**9.516**		0.812	0.016	0.065				
Phase I	C:N in POM < 10 µm	--	--	--	Chl *a* (0 – 17 m)	0.796	0.019	0.076				
Phase II		**0.009**	**0.982**	**105.800**		**0.020**	**0.780**	**14.180**				
Phase III		0.164	0.699	4.643		**0.022**	**0.766**	**13.070**				
Phase I	N:P in total POM	0.707	0.039	0.163	Chl *a* (0 – 10 m)	0.227	0.337	2.037				
Phase II		0.848	0.010	0.042		**0.034**	**0.714**	**9.995**				
Phase III		0.397	0.184	0.900		**0.008**	**0.859**	**24.320**				
Phase I	C:P in total POM	0.507	0.117	0.529								
Phase II		0.582	0.082	0.358								
Phase III		0.056	0.641	7.133								
Phase I	C:BSi in total POM	0.989	0.000	0.000								
Phase II		0.127	0.480	3.695								
Phase III		0.307	0.255	1.370								

Table 4. Results of linear regression analyses of CO_2 and percentage contribution of phytoplankton groups to chlorophyll *a*.

Phytoplankton group	**Phase I**			**Phase II**			**Phase III**		
	p	Multiple R^2	F-statistic	*p*	Multiple R^2	F-statistic	*p*	Multiple R^2	F-statistic
Prasinophytes	0.645	0.058	0.248	0.095	0.543	4.751	**0.025**	**0.754**	**12.270**
Cryptophytes	0.995	0.001	0.004	0.463	0.141	0.657	*0.041*	*0.687*	*8.789*
Chlorophytes	0.631	0.063	0.269	0.244	0.317	1.860	**0.008**	**0.857**	**24.020**
Cyanobacteria	0.224	0.341	2.067	0.421	0.167	0.803	0.153	0.437	3.110
Diatoms	0.866	0.008	0.324	0.515	0.113	0.508	*0.009*	*0.849*	*22.560*
Euglenophytes	0.962	0.001	0.003	0.438	0.156	0.741	0.976	0.000	0.001

Table 5. Summary of linear regression analyses done on absolute concentrations of phytoplankton pigments for the three experiment phases in different size fractions. Bold indicated significant positive effect and italics indicates significant negative effect of CO_2 concentration. ND indicates pigment was not detected. Where no pigment was detected in any phase in any size fraction, results were not included in this table.

Pigment	Size fraction	Phase I			Phase II			Phase III		
		p	Multiple R^2	F-statistic	*p*	Multiple R^2	F-statistic	*p*	Multiple R^2	F-statistic
Chlorophyll *a*	total	0.470	0.137	0.636	**0.008**	**0.854**	**23.440**	0.081	0.573	5.377
	< 2 µm	**0.014**	**0.815**	**17.650**	0.658	0.053	0.228	0.659	0.057	0.227
	> 20 µm	**0.009**	**0.850**	**22.720**	**0.011**	**0.836**	**20.440**	0.273	0.288	1.616
Chlorophyll *b*	total	0.143	0.454	3.321	**0.034**	**0.713**	**9.920**	0.885	0.006	0.024
	< 2 µm	0.815	0.015	0.063	0.726	0.034	0.141	0.369	0.204	1.025
	> 20 µm	**0.001**	**0.944**	**66.940**	**0.004**	**0.896**	**34.320**	ND	ND	ND
Chlorophyll C2	total	0.283	0.278	1.538	*0.026*	*0.750*	*12.010*	0.371	0.202	1.015
	< 2 µm	0.877	0.007	0.027	0.437	0.157	0.745	0.876	0.007	0.028
	> 20 µm	ND	ND	ND	0.094	0.544	4.765	ND	ND	ND
Canthaxanthin	total	**0.031**	**0.726**	**10.590**	ND	ND	ND	ND	ND	ND
	< 2 µm	0.078	0.582	5.576	ND	ND	ND	0.973	ND	0.001
	> 20 µm	ND	ND	ND	ND	ND	ND	ND	ND	ND
Fucoxanthin	total	0.876	0.007	0.028	0.420	0.168	0.807	0.371	0.202	1.012
	< 2 µm	0.131	0.472	3.581	0.374	0.200	1.000	0.257	0.304	1.743
	> 20 µm	0.649	0.057	0.242	0.370	0.201	1.020	**0.037**	**0.705**	**9.560**
Myoxoxanthophyll	total	0.056	0.642	7.157	0.755	0.027	0.112	ND	ND	ND
	< 2 µm	ND	ND	ND	ND	ND	ND	ND	ND	ND
	> 20 µm	ND	ND	ND	ND	ND	ND	ND	ND	ND
Neoxanthin	total	0.940	0.002	0.007	**0.006**	**0.880**	**29.310**	0.089	0.555	4.986
	< 2 µm	**0.030**	**0.730**	**10.820**	0.660	0.053	0.225	0.820	0.015	0.059
	> 20 µm	**0.005**	**0.890**	**32.470**	**0.003**	**0.907**	**39.090**	ND	ND	ND
Prasinoxanthin	total	**0.040**	**0.691**	**8.947**	**0.001**	**0.945**	**68.540**	ND	ND	ND
	< 2 µm	0.517	0.112	0.504	0.072	0.595	5.883	0.503	0.119	0.539
	> 20 µm	**0.001**	**0.951**	**77.440**	**0.003**	**0.917**	**44.360**	ND	ND	ND
Violaxanthin	total	**0.030**	**0.731**	**10.840**	**0.002**	**0.929**	**52.580**	**0.035**	**0.711**	**9.839**
	< 2 µm	**0.017**	**0.797**	**15.710**	0.854	0.01ß	0.038	0.882	0.006	0.025
	> 20 µm	**0.002**	**0.926**	**49.770**	**0.002**	**0.925**	**49.480**	0.982	ND	0.001

Figure 1. Diagram of Kiel Off-Shore Mesocosm for future Ocean Simulations showing floating frame, mesocosm bag and attached sediment trap. Source: GEOMAR

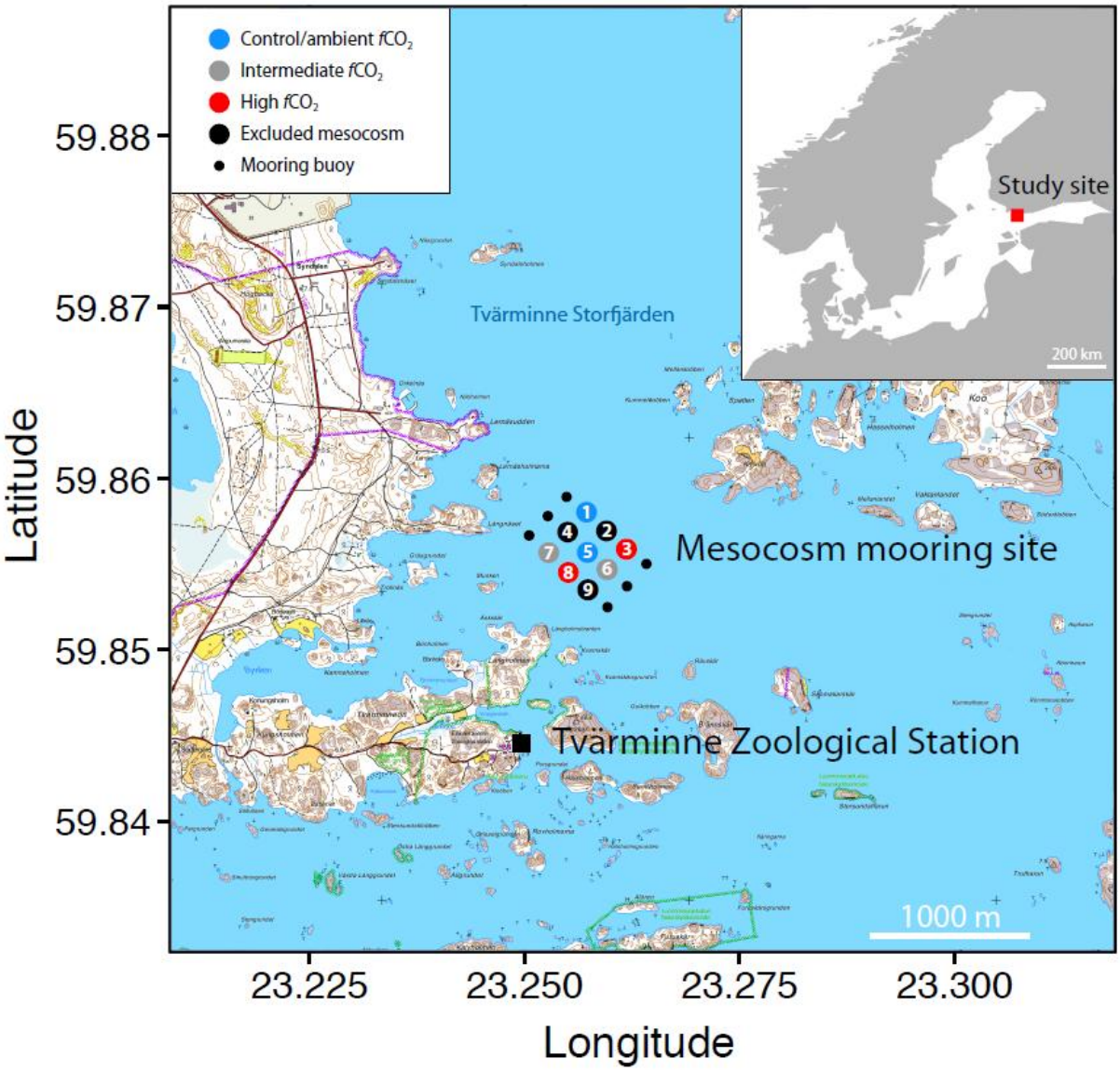

Figure 2. Map of study area (inset) and mesocosm mooring site in the Tvärminne Storfjärden, off the Hanko Peninsula close to the entrance to the Gulf of Finland in the Baltic Sea. Mesocosm representation is not to scale. Map contains data from the National Land Survey of Finland Topographic Database, accessed March 2015.

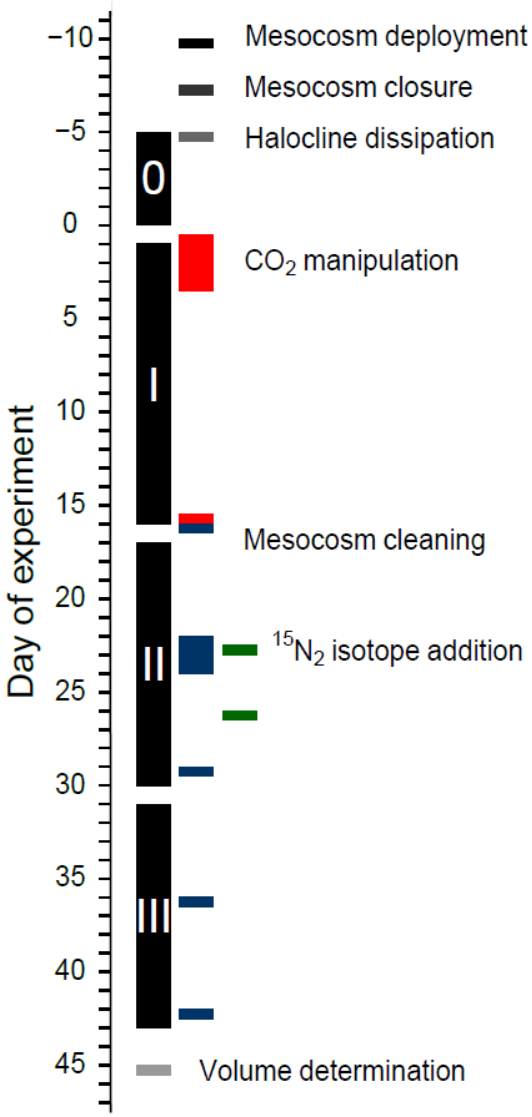

Figure 3. Experiment timeline indicating important activities such as CO_2 manipulations (red), cleaning (dark blue), phases (black labelled with 0, I, II and III for Phases 0, I, II and III respectively), volume determination (light grey) and isotope addition (dark green). Distinction of experimental phases is described in section 3.1.

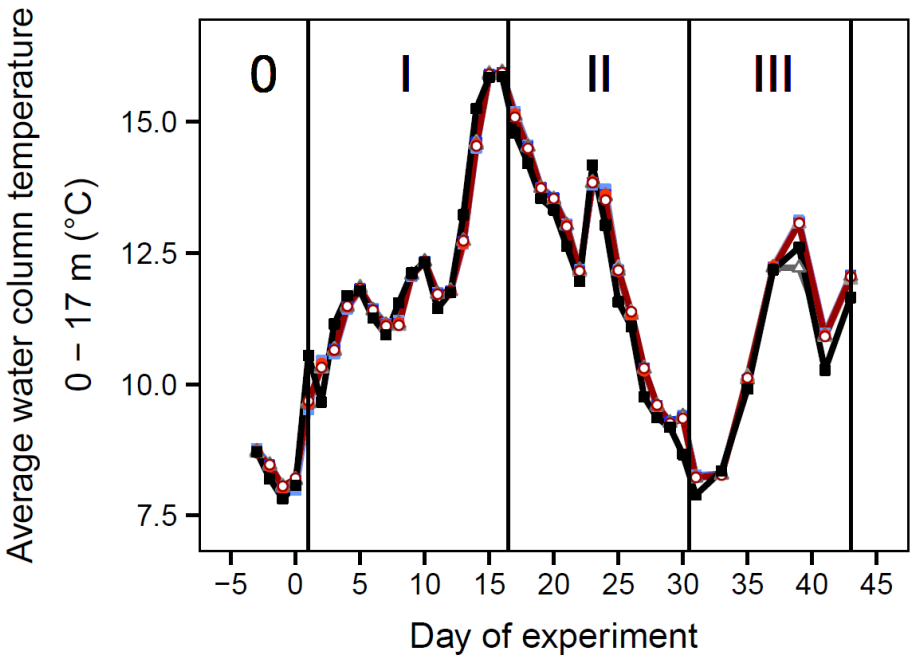

Figure 4. Variation in average water column temperature for all mesocosms and surrounding water during the study period. CO_2 enrichment (after *t0*) and temperature variations defined experimental phases. Phase 0 = no CO_2 treatments, Phase I = warming, Phase II = cooling, Phase III = 2nd warming phase until end of the experiment at *t43*. Colours and symbols are described in Table 1.

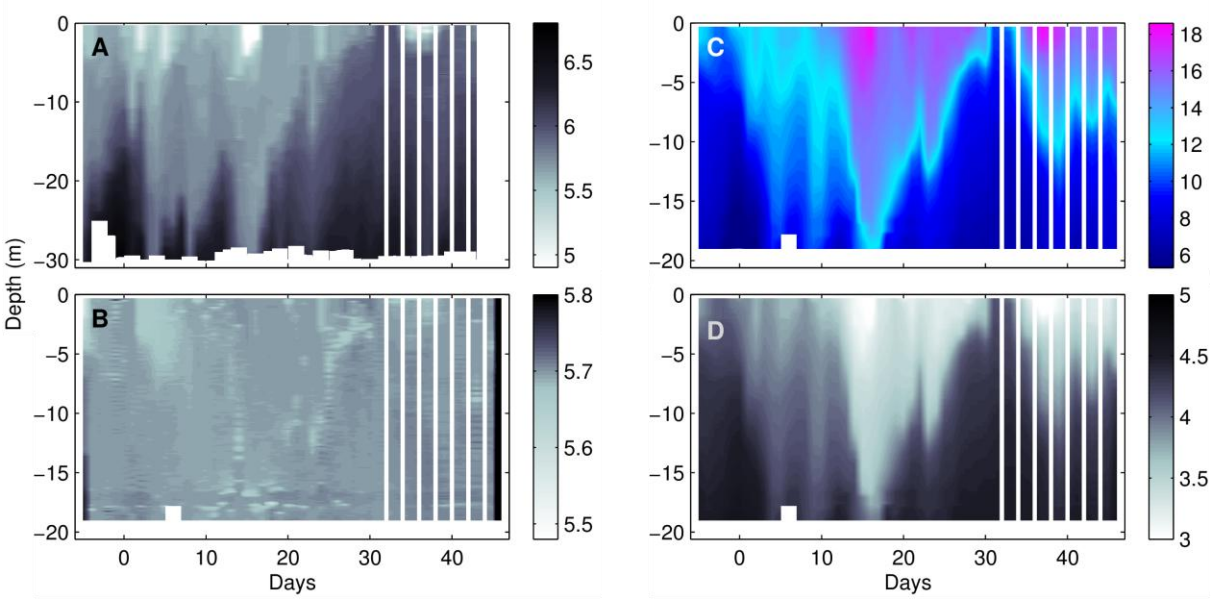

Figure 5. CTD profiles taken between *t-5* and *t46* for A) salinity of surrounding water (Baltic), and B) salinity, C) temperature (°C), and D) density anomaly of M8 (σ_T in kg m^{-3}). M8 profiles are representative for all mesocosms. White vertical lines indicate CTD profiles were taken every second day after *t31*.

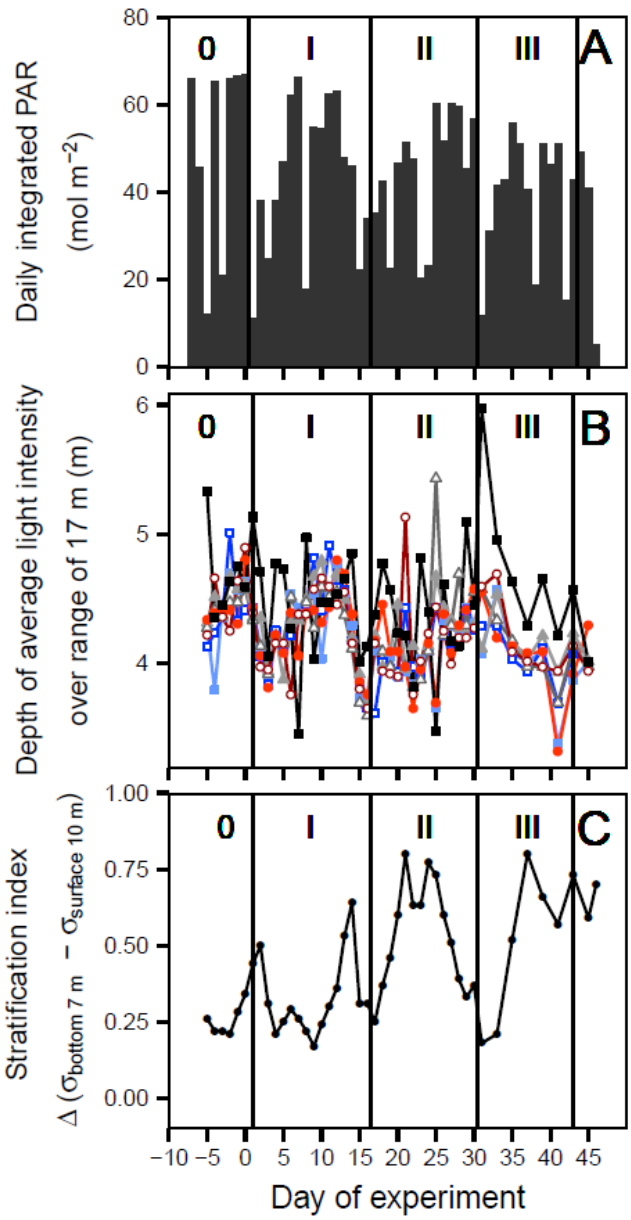

Figure 6. A) Daily integrated incoming photosynthetically active radiation (PAR) measured by a unobstructed sensor on land during the study period, B) depth of average water column light intensity calculated from CTD PAR sensor profiles between 0 and 17 m deep, and C) stratification index calculated from σ_T difference between the top 10 m and bottom 7 m in M8 as representative for all mesocosms. Symbols and colours are described in Table 1.

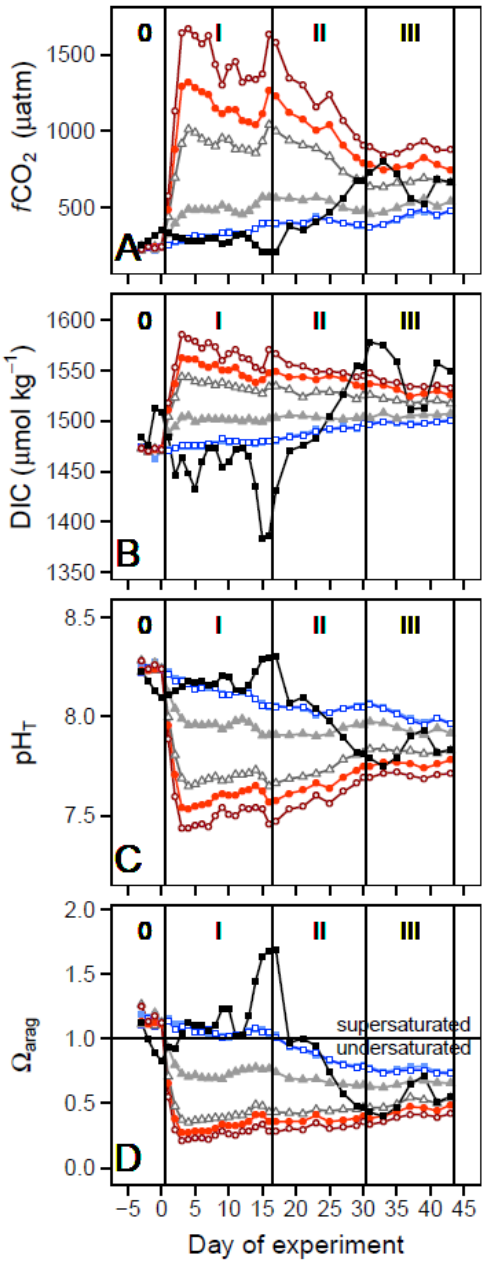

Figure 7. Dynamics in carbonate chemistry speciation with A) calculated fugacity of CO_2, B) measured dissolved inorganic carbon concentrations, C) measured pH on total scale and calculated for in-situ temperatures, and D) calculated saturation state (Ω) of calcium carbonate (aragonite). Ω_{arag} and fCO_2 were calculated from DIC and TA using the stoichiometric equilibrium constants for carbonic acid of Mehrbach et al. (1973) as refitted by Lueker et al. (2000). Colours and symbols are described in Table 1.

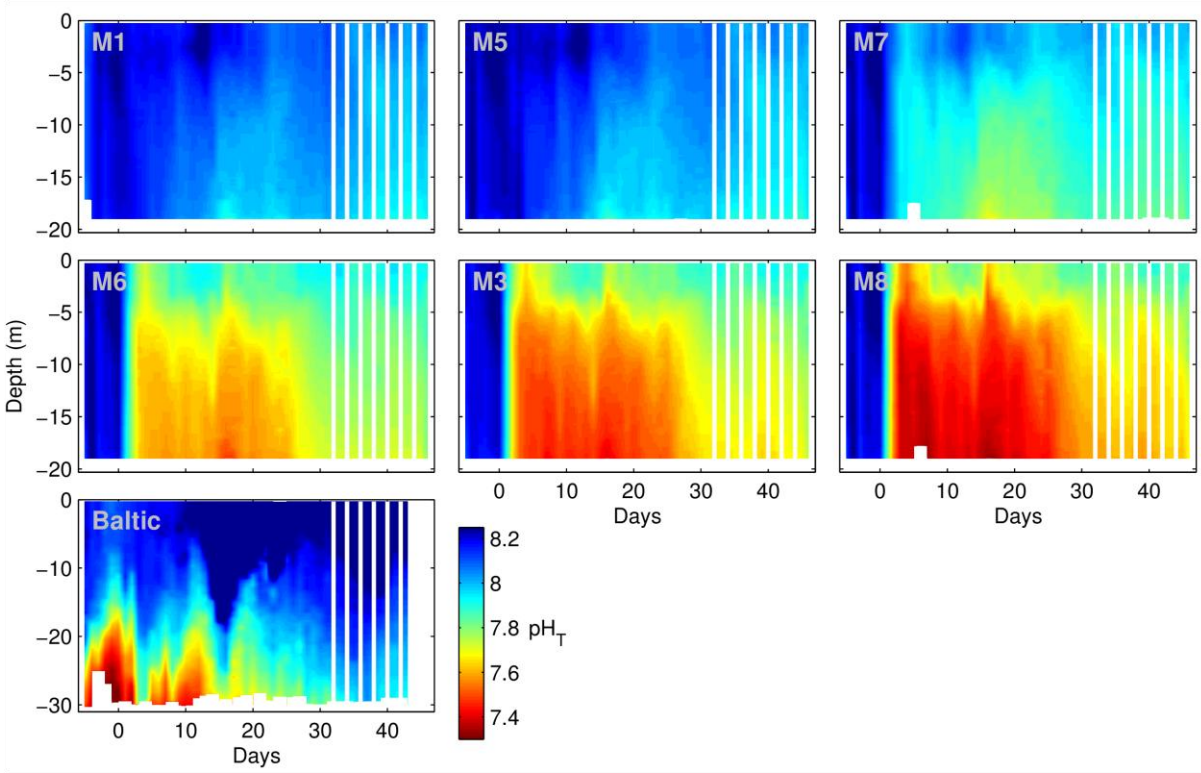

Figure 8.Vertical pH_T profiles taken using a pH sensor on a hand-operated CTD during the experiment in the mesocosms and in the surrounding water, here named 'Baltic'. For details of CTD operations and pH_T calculations, see section 2.5.1. White vertical lines indicate CTD profiles were taken every second day after *t31*.

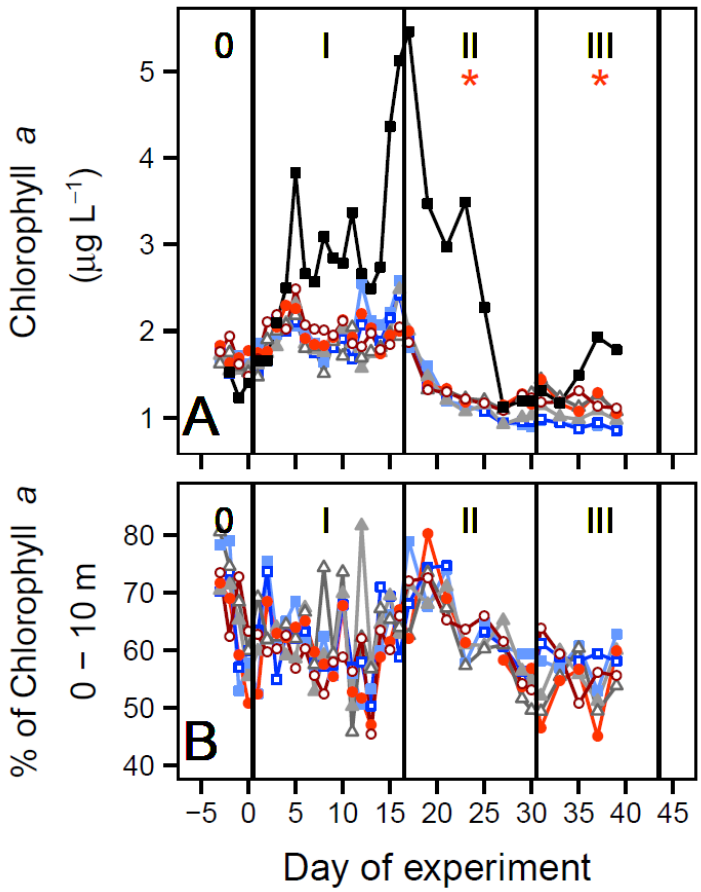

Figure 9. Temporal dynamics in A) chlorophyll *a* (0 – 17 m) including surrounding water and B) percent of total chlorophyll *a* in the upper 10 m. Colours and symbols are described in Table 1. Red asterisk denotes significant positive effect of CO_2 (* = $p < 0.05$).

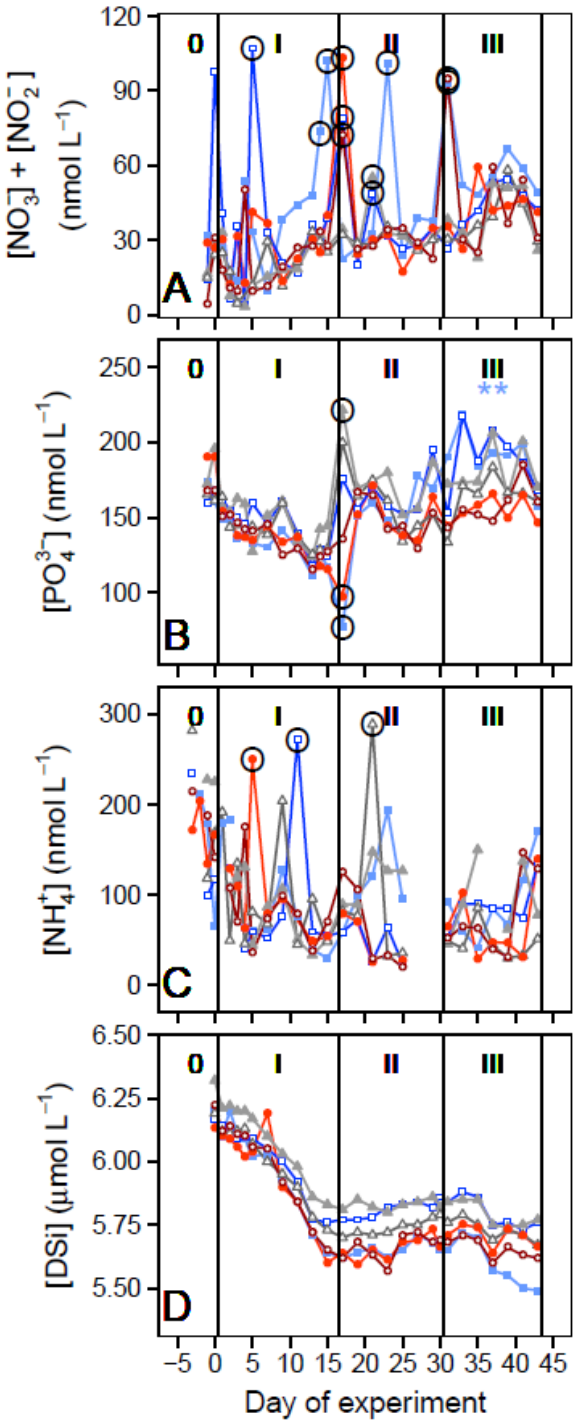

Figure 10. Temporal variation in concentrations of A) dissolved nitrate + nitrite, B) dissolved inorganic phosphate, C) ammonium, and D) dissolved silicate. Colours and symbols are described in Table 1. Blue asterisk denotes a statistically significant negative effect of CO_2 (** = $p < 0.01$). Outliers (Grubb's test; see methods) are indicated by black circles and were excluded from linear regression analyses.

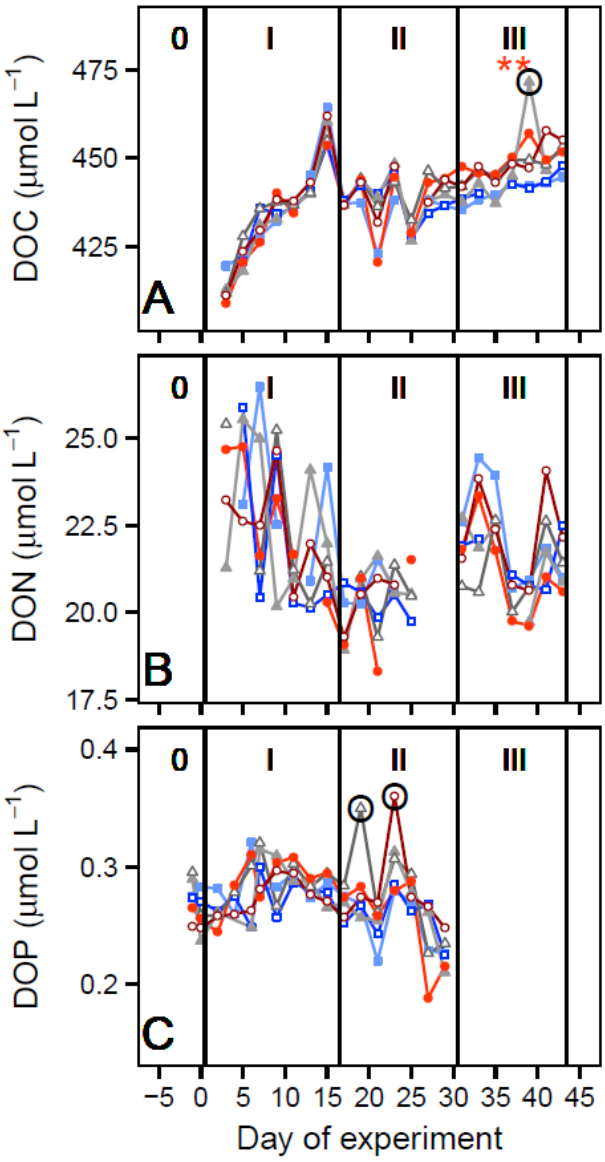

Figure 11. Temporal variation in concentrations of A) dissolved organic carbon, B) dissolved organic nitrogen, and C) dissolved organic phosphorus. CO_2 treatments are indicated by colours and symbols described in Table 1. Red asterisks denotes a statistically significant positive effect of CO_2 (** = $p < 0.01$). Outliers (Grubb's test; see methods) are indicated by black circles and were excluded from linear regression analyses.

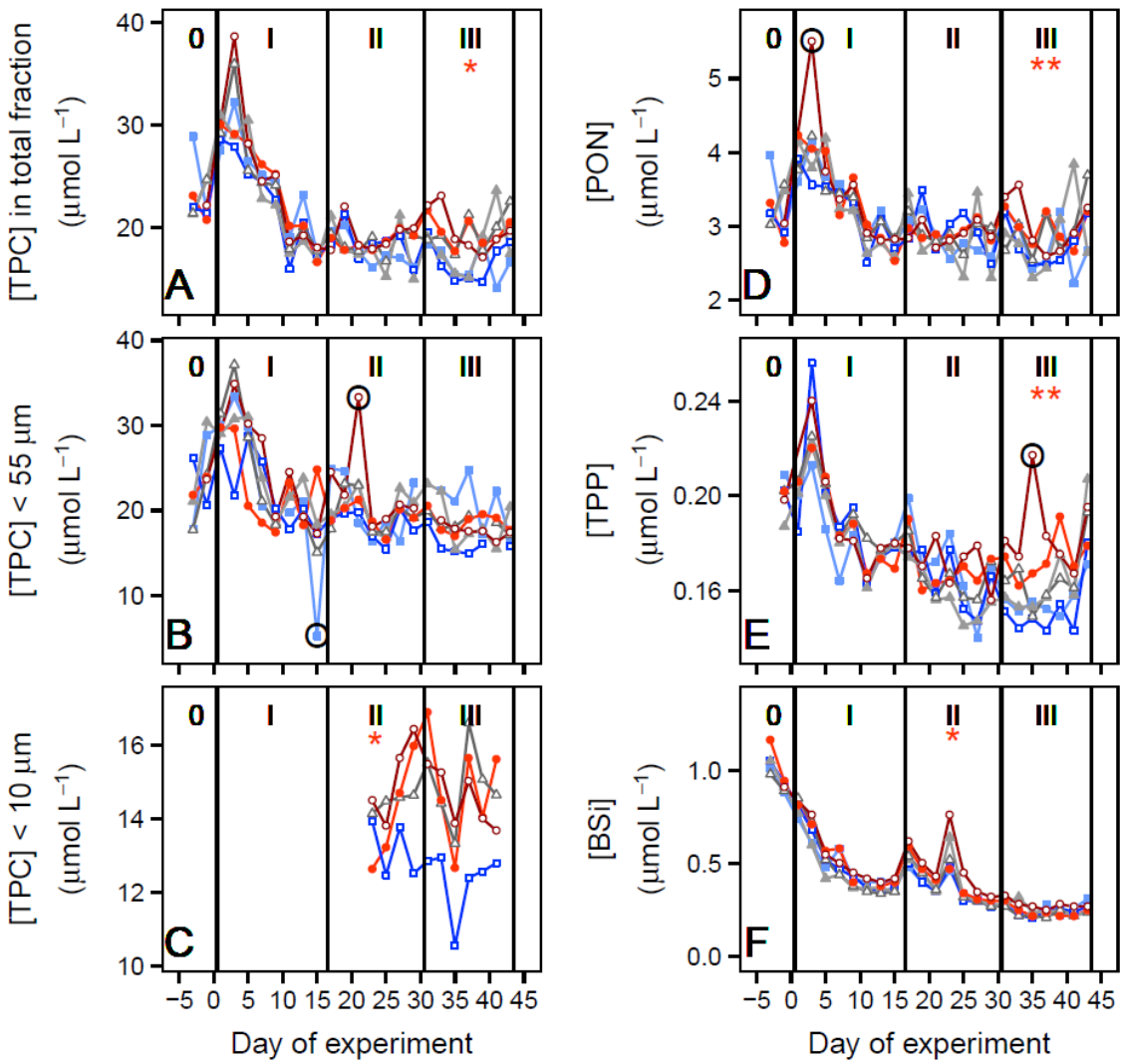

Figure 12. Temporal dynamics in concentrations of A) total particulate carbon, B) particulate carbon < 55 µm, C) particulate carbon < 10 µm, D) particulate organic nitrogen, E) total particulate phosphorus, and F) particulate biogenic silica. Colours and symbols are described in Table 1. Red asterisk denotes significant positive effect of CO_2 (* = $p < 0.05$, ** = $p < 0.01$). Outliers (Grubb's test; see methods) are indicated by black circles and were excluded from linear regression analyses.

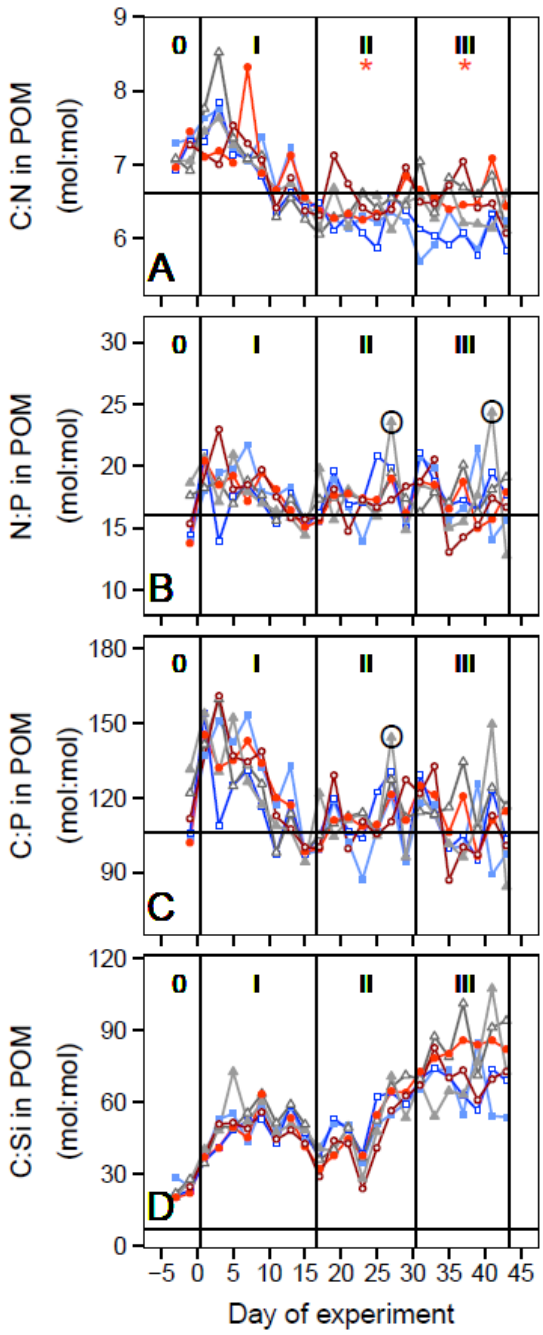

Figure 13. Temporal dynamics of elemental stoichiometry in particulate organic matter: A) carbon to nitrogen, B) nitrogen to phosphorus, C) carbon to phosphorus, D) carbon to biogenic silica. Horizontal lines indicate Redfield stoichiometry (C:N:P:Si = 106:16:1:15, Redfield (1958)). Colours and symbols for different treatments are described in Table 1. Red asterisk denotes significant positive effect of CO_2 (* = $p < 0.05$). Outliers (Grubb's test; see methods) are indicated by black circles and were excluded from linear regression analyses.

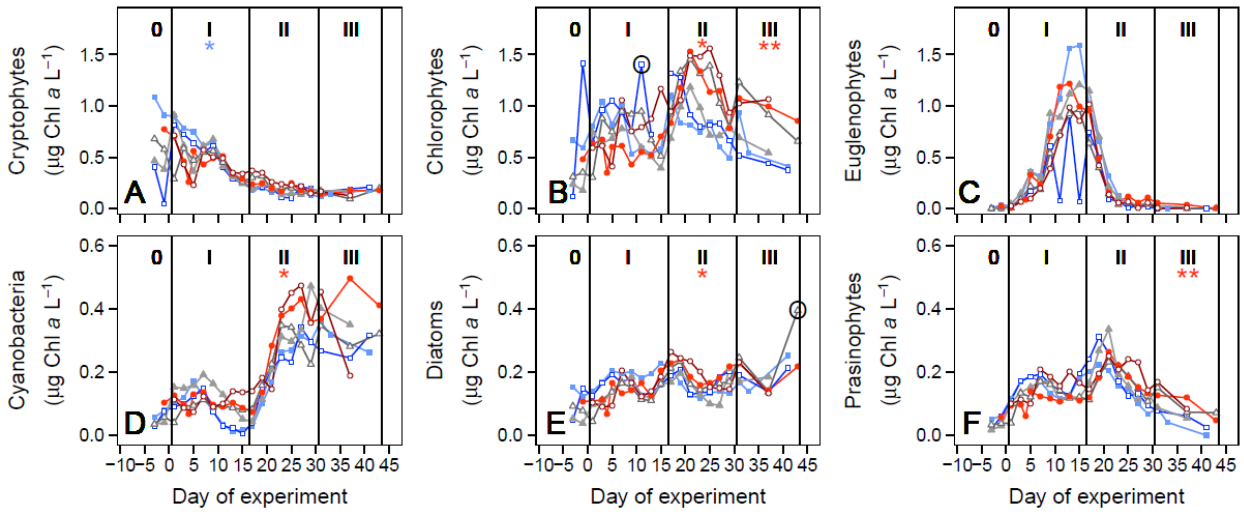

Figure 14. Contribution to total chlorophyll *a* by different phytoplankton groups as calculated by CHEMTAX from HPLC pigment analyses: A) cryptophytes, B) chlorophytes, C) euglenophytes, D) cyanobacteria, E) diatoms, and F) prasinophytes. Colours and symbols for each CO_2 treatment are described in Table 1. Red asterisk denotes significant positive effect and blue asterisk a significant negative effect of CO_2 (* = $p < 0.05$, ** = $p < 0.01$). Outliers are indicated by black circles and were excluded from linear regression analyses.

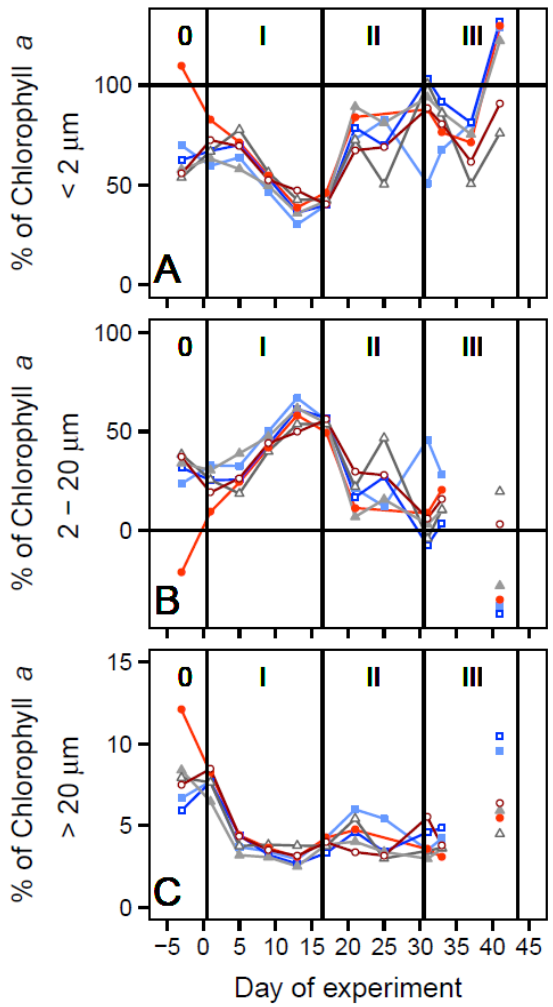

Figure 15. Relative contribution of different size fractions to total chlorophyll *a*. Size fraction 2 – 20 µm was calculated as a mass balance from total fraction and the two size fractions <2 µm and > 20 µm. Colours and symbols for different treatments are described in Table 1. Values larger than 100% or smaller than 0% are due to errors in mass balance calculation.

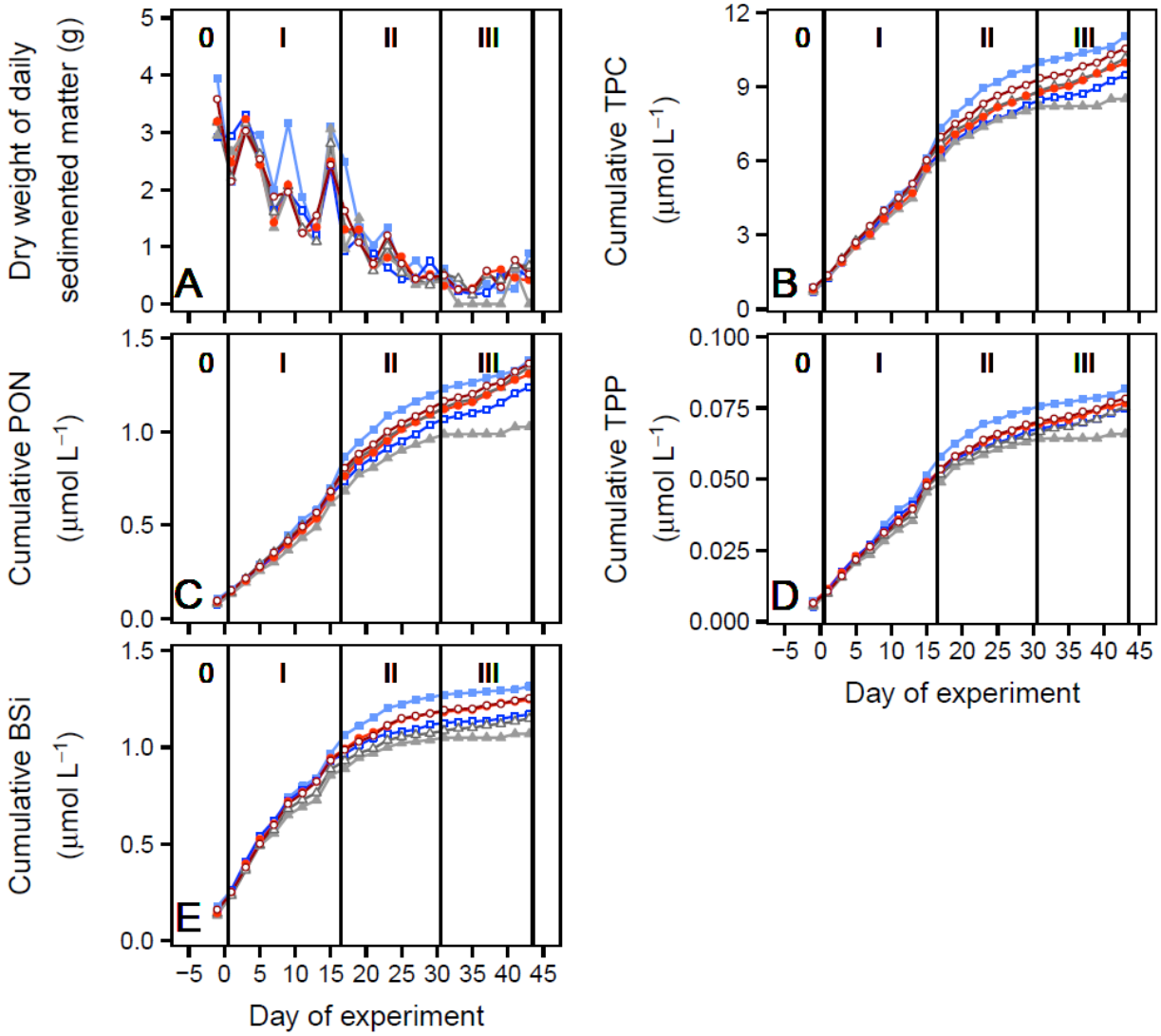

Figure 16. Temporal dynamics in A) collected sediment trap material mass and cumulative B) total particulate carbon, C) particulate organic nitrogen, D) total particulate phosphorus, and E) particulate biogenic silica. Concentrations in B-E were calculated based on individual mesocosm volumes determined at the end of the study. Colours and symbols for different treatments are described in Table 1.